3. Raman spectroscopy

Prehistory

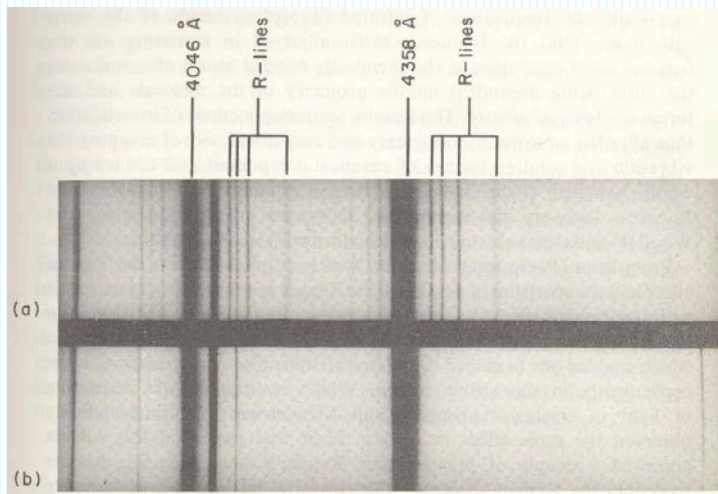|		
Compton effect	1923	X-ray photons/electrons
Smekal	1923	Inelastic scattering molecular analogue to Compton effect
Krames-Heisenberg	1925	Classical electromagnetic theory

History

C.V. Raman, R.K. Krisna	1928	CCl_4, C_6H_6
G. Landsberg, L. Mandelstam	1928	Quartz crystal

Name:
"feeble fluorescence"
"new radiation"
"Raman effect/scattering" (1930, Nobel prize)
"Smekal-Raman effect" (Germany)

It is a light scattering technique

Rayleigh Scattering
$\lambda_{scatter} = \lambda_{laser}$

Raman Scattering
$\lambda_{scatter} > \lambda_{laser}$

C.V. Raman won the Nobel Prize for Physics in 1930 for his work on the scattering of light and for the discovery of the effect named after him.

RAMAN'S SPECTROGRAPH
THE FIRST RAMAN SPECTRUM WAS OBTAINED WITH THIS SPECTROGRAPH IN 1928.

Provided by Prof. D. Mukherjee, Director of Indian Association for the Cultivation of Science

(a) The Raman spectrum of CCl$_4$ taken by C.V. Raman in 1928 (b) Comparison mercury spectrum.

Developments

| 1928-1962 | Excitation with low-pressure Hg-arc |
	435.8 nm (22938 cm^{-1})
	404.7 nm (24705 cm^{-1})
	sample 5-10 ml liquid
1962	Porto-Wood pulsed Rubin laser
1963	CW He-Ne laser
1963	CW Ar$^+$, Kr$^+$, Nd: YAG, Diode
1986	FT-Raman (B. Chase)
1992	Raman microscope (Ranishaw, Univ. Leeds)

Background

The early 1920s was a time of intense interest in the scattering of electromagnetic radiation by charged particles, The Compton effect, the name given to the quantum mechanical explanation of changes in wavelength of X-ray photons when scattered by electrons, was first documented in 1923. Almost immediately Smekal, in Germany, predicted the inelastic scattering of light by molecules in terms of an analogy to the Compton effect. There was a related prediction, in terms of c1assical electromagnetic theory, by Kramers and Heisenberg in, 1925. With this background, the experimental observation of what C. V. Raman in India called at first "feeble fluorescence" and later termed the "New Radiation" seems to have been almost inevitable. It is not surprising, therefore, that it was reported almost simultaneously by both Raman (1) and Landsberg and Mandelstam in Moscow (2) in 1928. The importance of this phenomenon was recognized by the award of the Nobel Prize in Physics to Raman in 1930, and it has been known as the Raman effect, Raman scattering, or Raman spectroscopy ever since.

The mercury lines at 435.8 nm (22,938 cm^{-1}) and 404.7 nm (24,705 cm^{-1}) from a low-pressure mercury arc were used to observe Raman scattering. These lines, however, may be absorbed by a number of compounds which have an electronic absorption band in this region.

The Raman Effect

When monochromatic light of energy $h\nu_0$ encounters matter (gas, solid, or liquid), there is a small probability that it will be scattered at the same frequency. If the object in question (e.g., a molecule) is much smaller than the wavelength of the light, the scattering is Rayleigh scattering, as shown in the figure below:
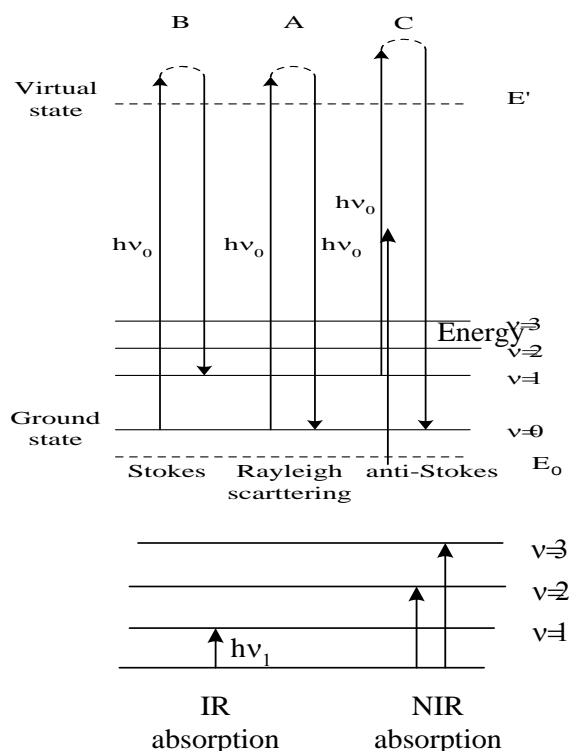
Spectroscopic transitions underlying several types of vibrational spectroscopy v_0 indicates laser frequency, while v is the vibrational quantum number. The virtual state is a short-lived distortion of the electron distribution by the electric field of the incident light.
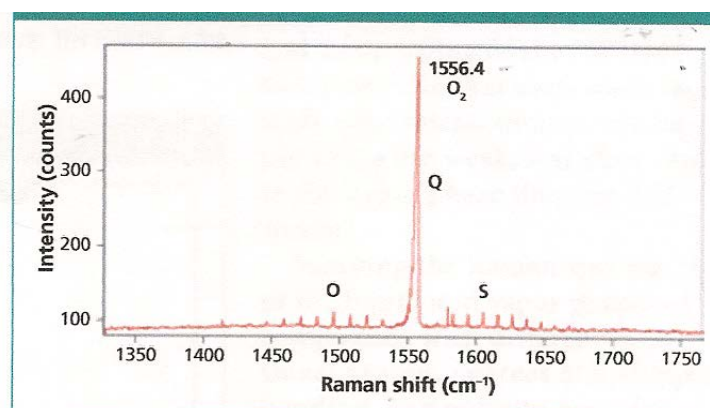
Stokes	$h(v_0 - v_1)$
Rayleigh	$h(v_0)$
Anti-Stokes	$h(v_0 + v_1)$

The Stokes and anti-Stokes Raman peaks are symmetrically positioned about the Rayleigh peak, but their intensities are very different except for low vibrational energies.
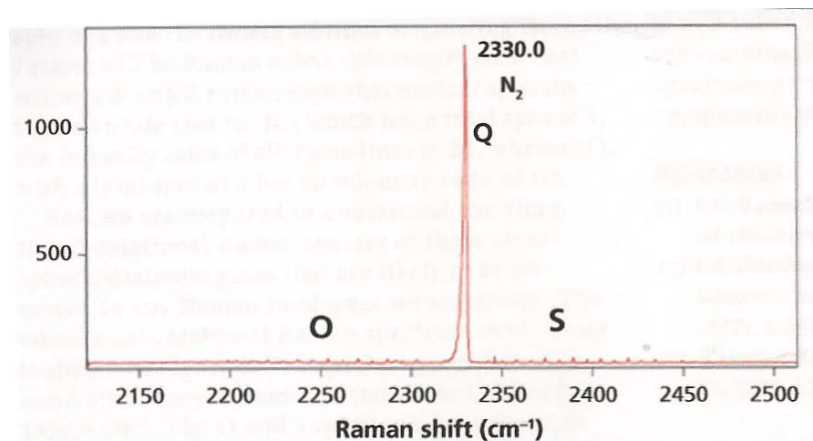
Raman scattering of simple homonuclear diatomic molecules
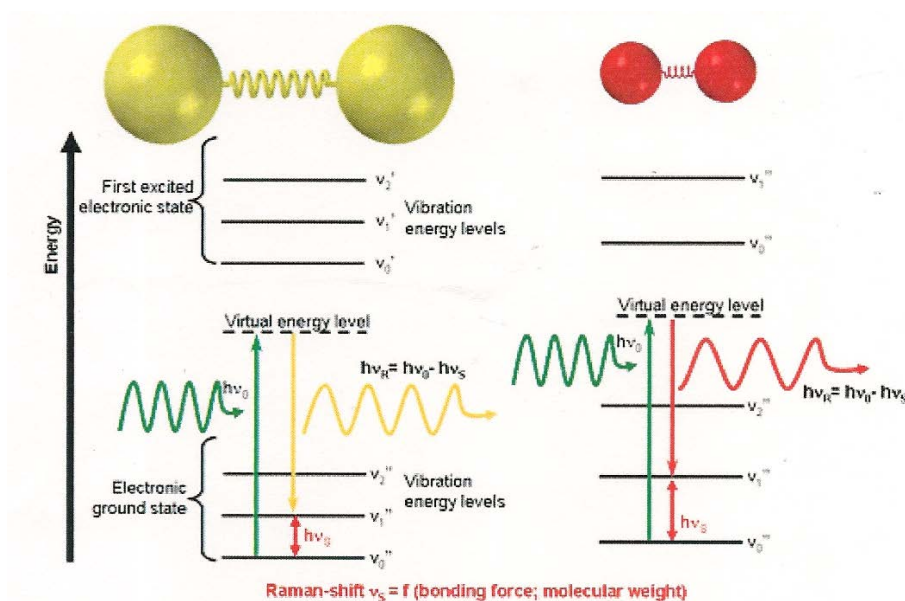
Raman scattering of O_2 (green) and N_2 (red) diatomic molecules

Raman spectrum of oxygen in air

Raman spectrum of nitrogen in air

Observed Raman frequencies of homonuclear diatomic molecules, ions and radicals

Molecule	$\tilde{\nu}_k/\mathrm{cm}^{-1}$
N_2	2331
O_2	1555
H_2	4156
D_2	2986
F_2	893
Cl_2	554
HF	3962

Species	State[a]	$\tilde{\nu}$
T_2[b]	Liquid	2458
Sn_2	Mat	188
Pb_2	Mat	112
P_2	Gas	775
As_2	Gas	421
O_2^-	Mat	1097
O_2^{2-}	Solid	794 738
S_2	Mat	718
S_2^-	Solid[d]	623
Se_2^-	Solid[d]	349
F_2^-	Mat	475

Species	State[a]	$\tilde{\nu}$
Cl_2[c]	Mat	546
Cl_2^-[c]	Mat	247
Br_2^+	Sol'n	360
Br_2	Gas	319
I_2^+	Sol'n	238
I_2	Gas	213
I_2^-	Mat	115
Ag_2	Mat	194
Zn_2	Mat	80
Cd_2	Mat	58

Bonding parameters of O_2 and its ions

Species	Bond Order	Bond Distance (Å)[a]	Bond Energy (Kcal/mole)[a]	$\nu(O_2)$ (cm^{-1})	Force Constant (mdyn/Å)
O_2^+	2.5	1.123	149.4	1876	16.59
O_2	2.0	1.207	117.2	1580	11.76
O_2^-	1.5	1.280	—	1094[b]	5.67
O_2^{2-}	1.0	1.49	48.8	791/736[b,c]	2.76

[a]Ref. 85

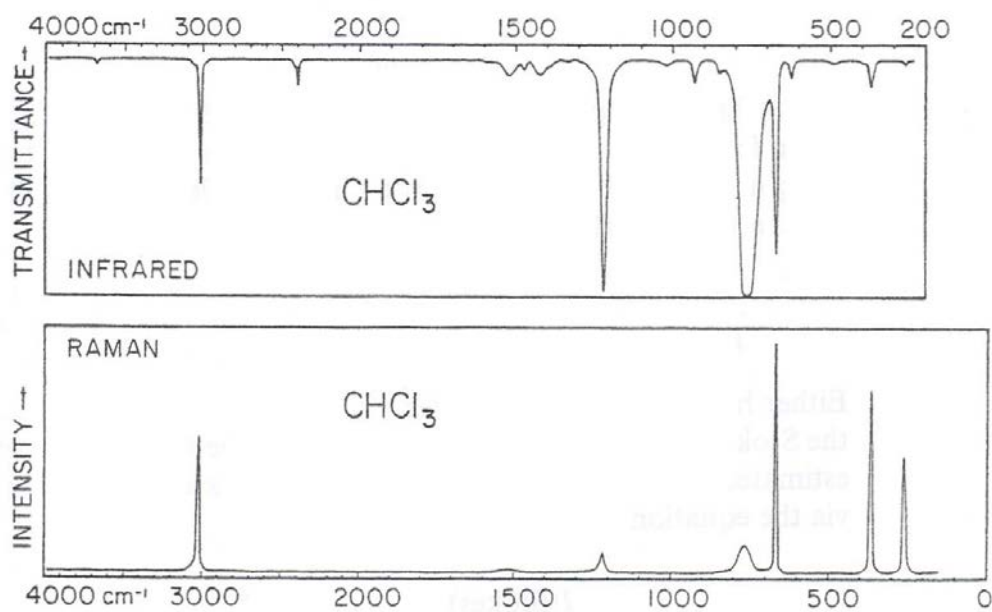134

Raman spectroscopy of simple molecules

Anti-Stokes   **Stokes**
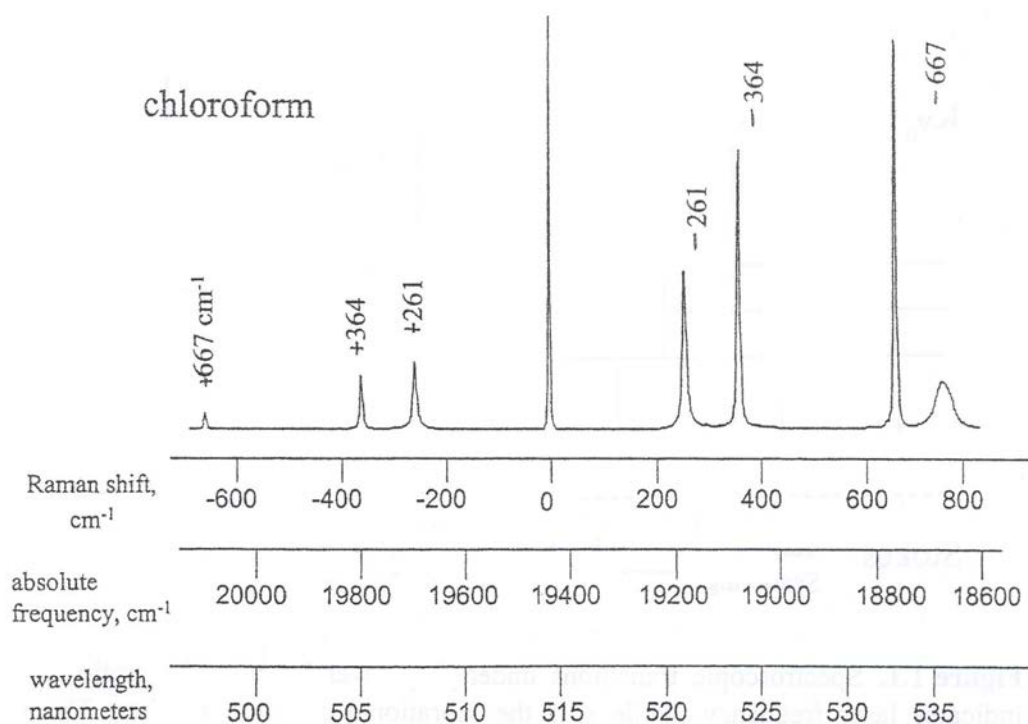
Raman spectrum of room-temperature chloroform obtained with 514.5 nm light.

Infrared and Raman spectra of chloroform

- Symmetrical vibrations show stronger Raman bands
- Asymmetric vibrations are stronger in IR

- Combination and overtones are stronger in IR

 Temperature measurements

Either high or low temperatures can be determined by measuring both the Stokes and anti-Stokes Raman spectra. The temperature of the sample is estimated from the intensity ratios of the Stokes and anti-Stokes Raman lines via the equation

$$\frac{I(Stokes)}{I(anti-Stokes)} = \frac{(v_0 - v_m)^4}{(v_0 + v_m)^4} \exp\left\{ hcv_m / kT \right\}$$

where v_0 is the wavenumber of the laser line, v_m is the wavenumber of a band of the solvent or sample, h is Planck's constant, c is the velocity of light, k is Boltzmann's constant, and T is absolute temperature. A more convenient equation may be written as

$$T = \frac{-v_m \, x 1.43879}{\ln\dfrac{I(anti-Stokes)}{I(Stokes)} + 4 \ln\dfrac{(v_0 - v_m)}{(v_0 + v_m)}}$$

However, this equation is not applicable when anti-Stokes lines are very weak. It should be noted that these equations are applicable only for the spectra obtained under off-resonance conditions.

Fluorescence problem

Fluorescence is not a scattering process, and fluorescence emission from most liquids and solids does not have the vibrational fine structure. Even weak fluorescence can be much stronger than Raman scattering, easily overwhelming the weak Raman signal.

As a phenomenon, fluorescence is approximately $10^6 - 10^8$ times stronger than Raman scattering. Often when one tries to excite a Raman spectrum, fluorescence is the only phenomenon observed. Trace impurities, coatings on polymers, additives, natural and biological samples etc., may fluoresce so strongly that it is impossible to observe the Raman spectrum of a major

component. The use of UV or near-IR excitation has proved to be effective in reducing fluorescence
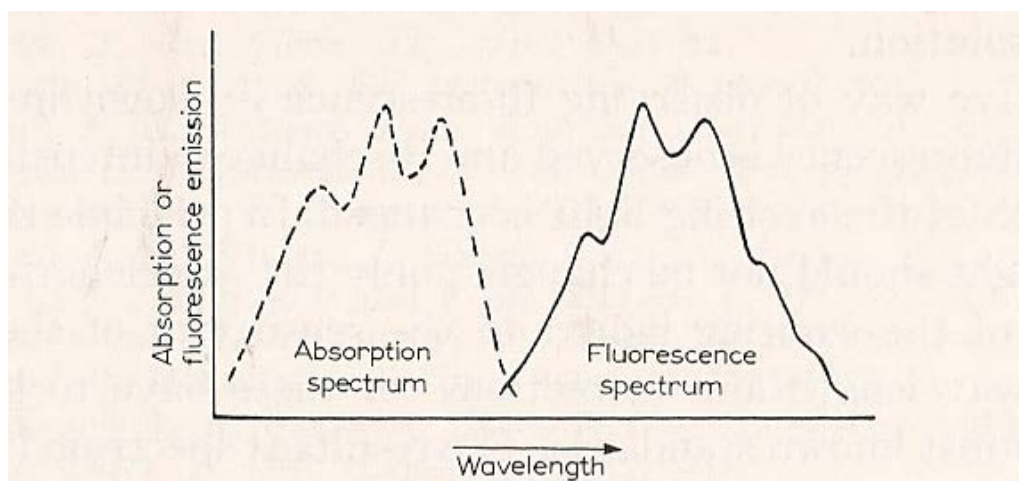
Comparison of absorbance and fluorescence

Comparison of cross sections (σ)

	σ (cm^2/molecule)
Raman	~10^{-30}
IR	~10^{-20}
Fluorescence	~10^{-10}

Fluorescence eliminations:

- purification of the sample;

- "burning" with high power laser beam;

- shifting ν_0 to longer (NIR) or shorter (UV) wavelength;

- addition of quenching agents (KI, HgCl$_2$, HgBr$_2$)

- repetitive scan with background subtraction

- using pulsed laser

        lifetime of Raman transition: $10^{-12} – 10^{-13}$ s

        lifetime of fluorescence: $10^{-7} – 10^{-9}$ s

Classical theory of Raman Effect, molecular polarization

If a molecule is placed in the electric field of electromagnetic radiation than the e1ectrons are displaced relative to the protons and the polarized molecule has an induced dipole moment. The induced dipole moment, μ, divided by the strength of the electric field E causing the induced dipole moment, is the polarizability α

$$\mu/E = \alpha$$

The polarizability can be looked on as the deformability of the electron cloud of the molecule by the electric field. *In order for a molecular vibration to be Raman active, the vibration must be accompanied by a change in the polarizability of the molecule.*

When a sample of such molecules is subjected to a beam of radiation of frequency v_0 the electric field experienced by each molecule varies:

$$E = E_0 \cos 2\pi v_0 t$$

and thus the induced dipole also undergoes oscillations of frequency v_0:

$$\mu = \alpha E = \alpha E_0 \cos 2\pi v_0 t \qquad (3.3)$$

Such an oscillating dipole emits radiation of its own oscillation frequency and we have immediately in Eq. (3.3) the classical explanation of Rayleigh scattering.

If, in addition, the molecule undergoes some internal motion, such as vibration or rotation, which *changes the polarizability* periodically, then for small displacements polarizability can be expanded in a Taylor series as

$$\alpha = \alpha_0 + \frac{\partial \alpha}{\partial Q} Q + ...$$

where α_0 is the equilibrium polarizability, Q is a normal coordinate (which is $r - r_e$ in the diatomic case), and $\partial \alpha / \partial Q$ is the rate of change of polarizability with respect to Q measured at the equilibrium configuration. Higher order terms are neglected in the harmonic approximation. The normal coordinate Q varies periodically

$$Q = Q_0 \cos 2\pi \nu_v t$$

where ν_v is the frequency of the normal coordinate vibration and Q_0 is a constant, the maximum value for Q. Combining the last two equation

$$\alpha = \alpha_0 + \frac{\partial \alpha}{\partial Q} Q_0 \cos 2\pi \nu_v t$$

The substitution of this value for α into Eq. 3.3 yields

$$\mu = \alpha_0 E_0 \cos 2\pi \nu t + \frac{\partial \alpha}{\partial Q} Q_0 E_0 (\cos 2\pi \nu_v t)(\cos 2\pi \nu_v t)$$

Making use of a trigonometric identity we can write

$$\mu = \alpha_0 E_0 \cos 2\pi \nu t + \frac{\partial \alpha}{\partial Q} \frac{Q_0 E_0}{2} \left[\cos 2\pi (\nu - \nu_v) t + \cos 2\pi (\nu + \nu_v) t \right]$$

From the above Eq.:
- Polarization and scattering (both Rayleigh and Raman) intensities are linear with the laser intensity *(E0)*;
- Only vibrations that change the polarizability $(\delta \alpha / \delta Q \neq 0)$ yield Raman scattering.

Polarization of Raman scattering

The oscillating induced dipole moment is

$$\mu = \alpha E = \alpha E_0 \, cos2\pi vt,$$

where the proportionality constant α is known as the polarizability. Classical theory gives the average rate of total radiation as

$$I = \frac{16\pi^4}{3c^3} v^4 \mu_0^2$$

where μ_0 is the amplitude of μ. For this case the scattered radiation has the same frequency as the incident.

The expression for μ can be rewritten in terms of Cartesian components; in its most general form

$$\mu_x = \alpha_{xx}E_x + \alpha_{xy}E_y + \alpha_{xz}E_z$$

$$\mu_y = \alpha_{yx}E_x + \alpha_{yy}E_y + \alpha_{yz}E_z$$

$$\mu_z = \alpha_{zx}E_x + \alpha_{zy}E_y + \alpha_{zz}E_z,$$

and this can be rewritten as a matrix equation $\mu = \alpha E$, that is,

$$\begin{bmatrix} \mu_x \\ \mu_y \\ \mu_z \end{bmatrix} = \begin{bmatrix} \alpha_{xx} & \alpha_{xy} & \alpha_{xz} \\ \alpha_{yx} & \alpha_{yy} & \alpha_{yz} \\ \alpha_{zx} & \alpha_{zy} & \alpha_{zz} \end{bmatrix} \begin{bmatrix} E_x \\ E_y \\ E_z \end{bmatrix}$$

For almost every case, α is a symmetric matrix $(\alpha_{xy} = \alpha_{yx},$ etc.$)$.

Depolarization Ratio

Let the direction of propagation of the incident radiation be the z axis and the direction of observation be perpendicular to the z axis in the xy plane. The depolarization ratio ρ is defined as the ratio of the intensity of scattered light polarized perpendicular to the xy plane $I\perp$ to that polarized parallel to the xy plane $I_\parallel$.

$$\rho = \frac{I_\perp}{I_\parallel}$$

Measurements of depolarization ratios

A molecule situated at the origin is irradiated from the y-direction with plane polarized light whose electric vector oscillates on the *yz-plane (E_z)*. If one observes scattered radiation from the x-direction, and measures the intensities in the $y(I_y)$ and $z(I_z)$-directions using an analyzer, the depolarization ratio *(ρ_p)* measured by polarized light *(p)* is defined by

$$\rho_p = \frac{I_\perp(I_y)}{I_{II}(I_z)}$$
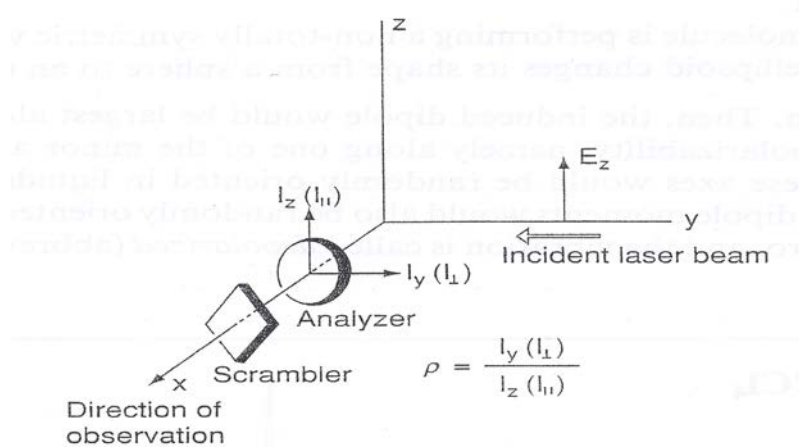
Irradiation of sample from the y-direction with plane polarized light, with the electronic vector in the z-direction.

Suppose that a tetrahedral molecule such as $CC1_4$ is irradiated by plane polarized light *(E_z)*. If the molecule is performing the totally symmetric vibration, the polarizability ellipsoid is always sphere-like; namely, the molecule is polarized equally in every direction. Under such a circumstance, $I\bot(I_y) = 0$ Thus, $\rho_p = 0$. Such a vibration is called *polarized* (abbreviated as *p*).

If the molecule is performing a non-totally symmetric vibration, the polarizability ellipsoid changes its shape from a sphere to an ellipsoid during the vibration. Then, the induced dipole would be largest along the direction of largest polarizability, namely along one of the minor axes of the ellipsoid. In this case, the ρ_p is nonzero, and the vibration is called *depolarized* (abbreviated as *dp*).
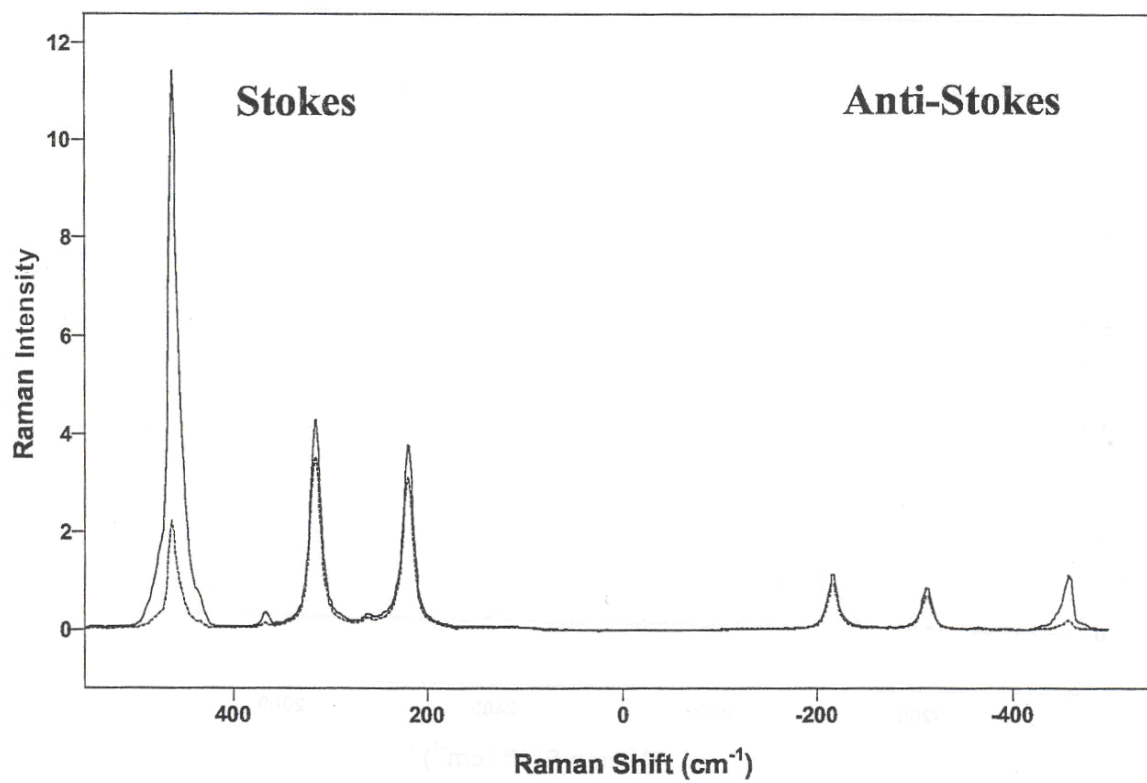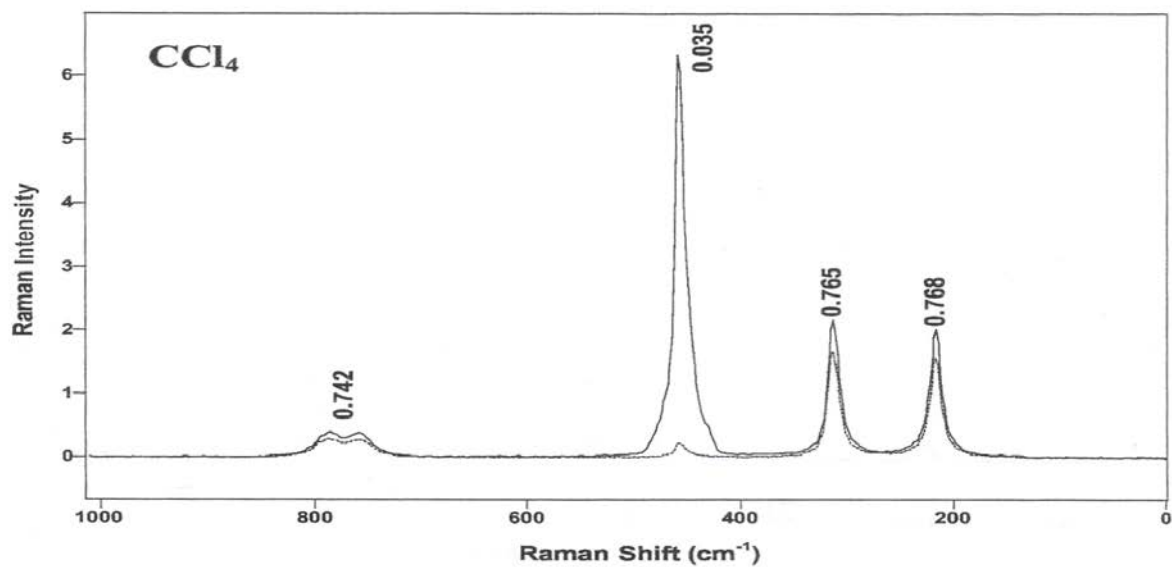
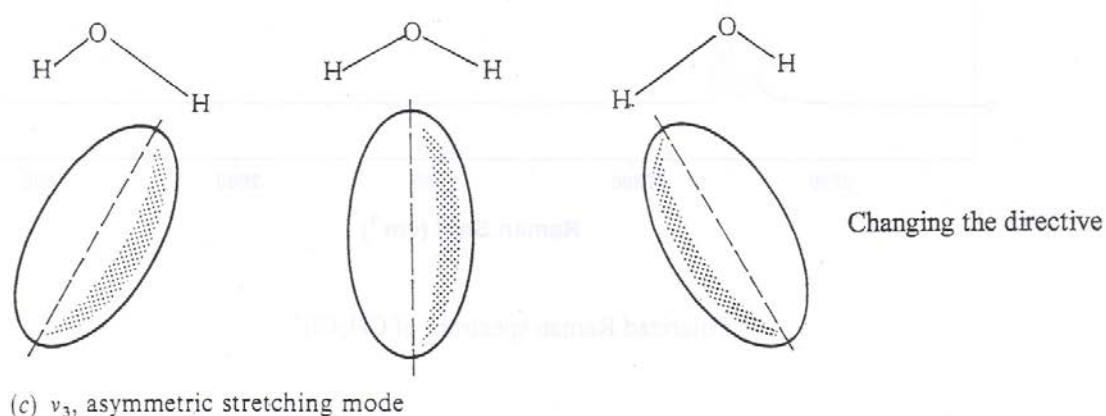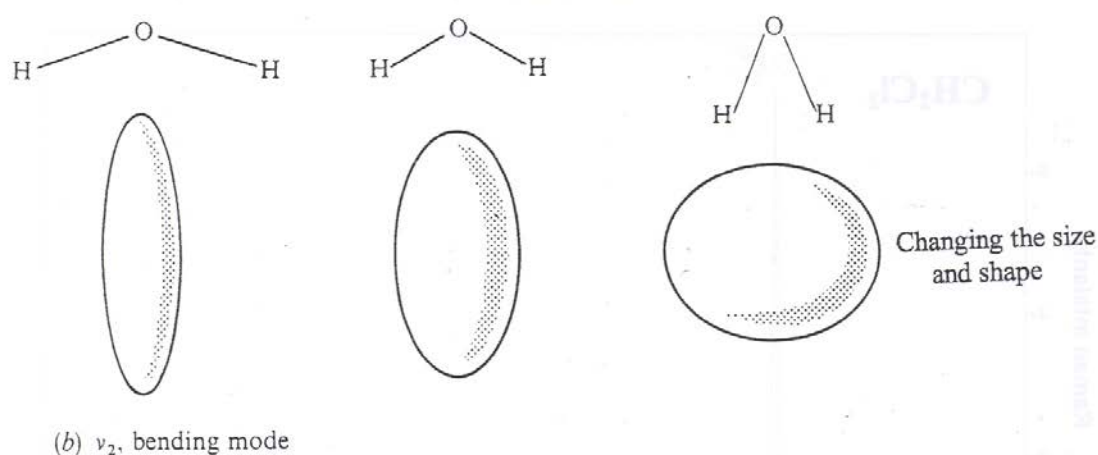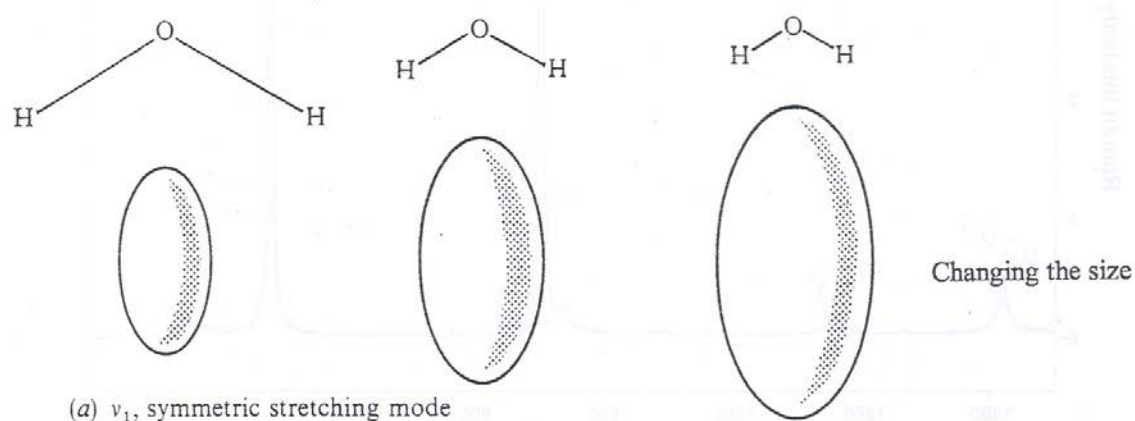**Polarized Stokes and anti-Stokes Raman spectrum of CCl₄**
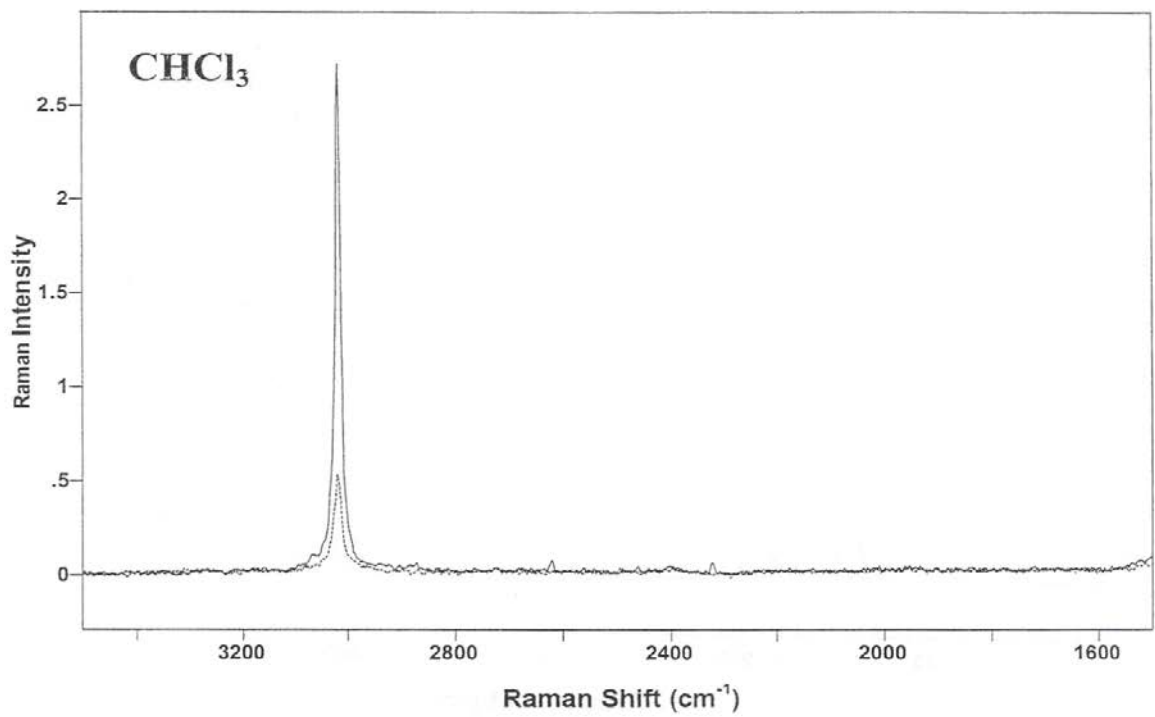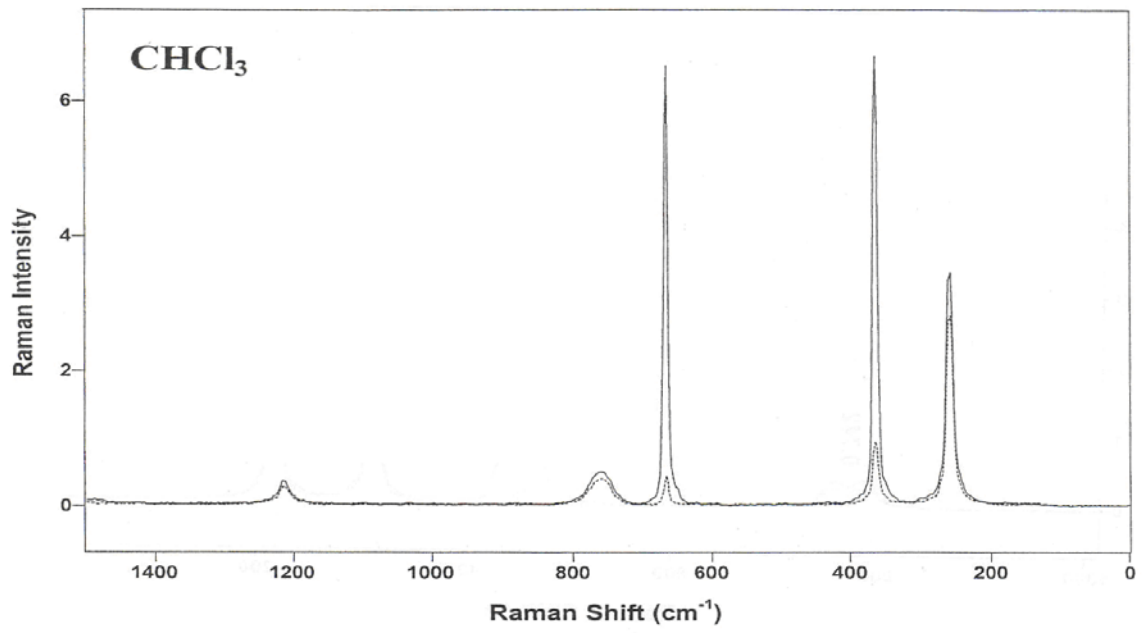
**Polarized Raman spectrum of CHCl₃**

143
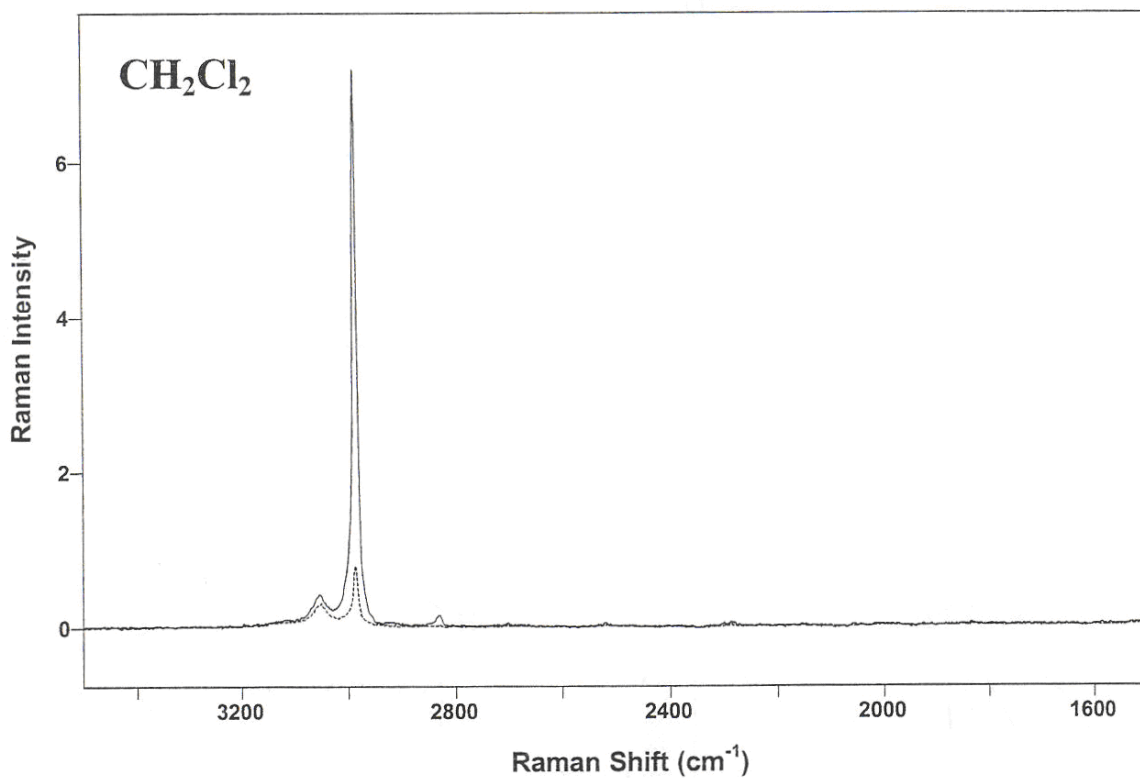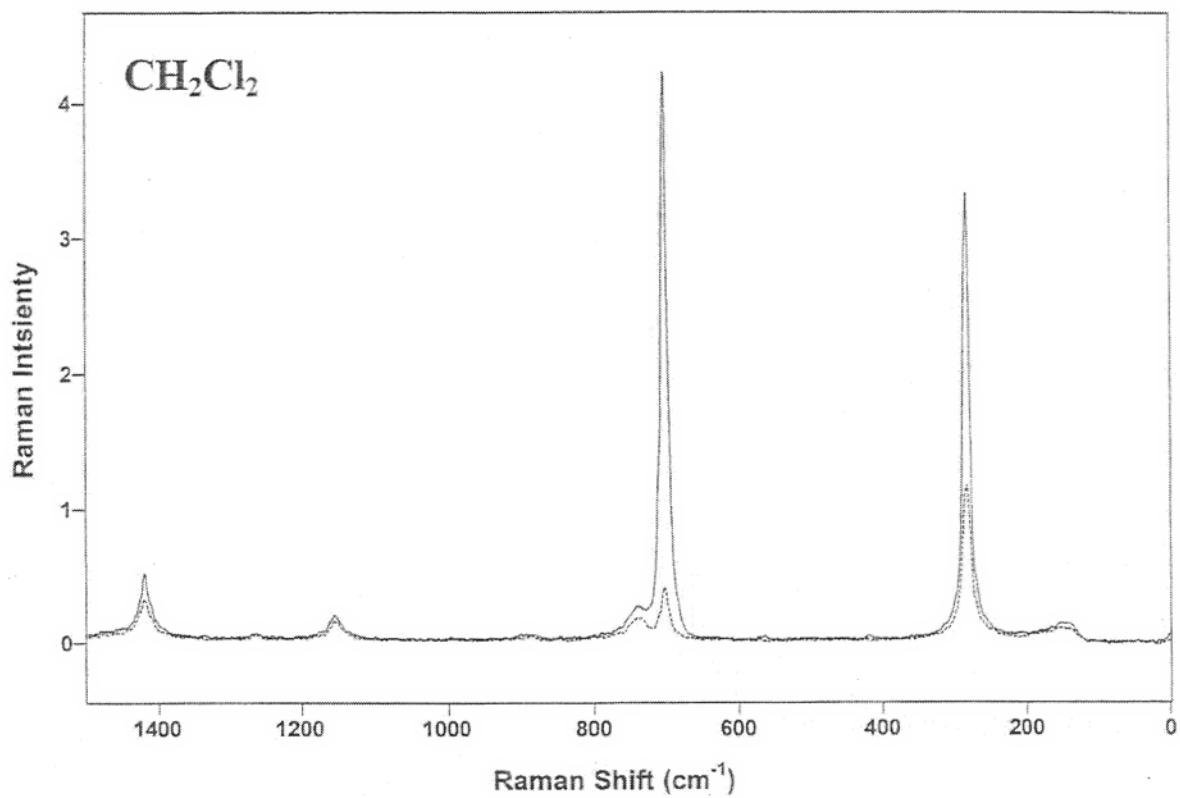
Polarized Raman spectrum of CH₂Cl₂

Vibrational Raman spectra

Which vibrational modes exhibit Raman activity?
Water molecule with its polarizability ellipsoids:

(a) v_1, symmetric stretching mode

Changing the size

(b) v_2, bending mode

Changing the size and shape

(c) v_3, asymmetric stretching mode

Changing the directive

The change in size, shape, or direction of the polarizability ellipsoid of the water molecule during each of its three vibrational modes. The centre column shows the equilibrium position of the molecule while to right and left are the extremes of each vibration.

Now consider the linear triatomic molecule CO_2, whose three fundamental vibrational modes have been shown in the figure below. We illustrate the extreme and equilibrium configurations of the molecule and their approximate polarizability ellipsoids..

(a) v_1, symmetric stretching mode

(b) v_2, bending mode

(c) v_3, asymmetric stretching mode
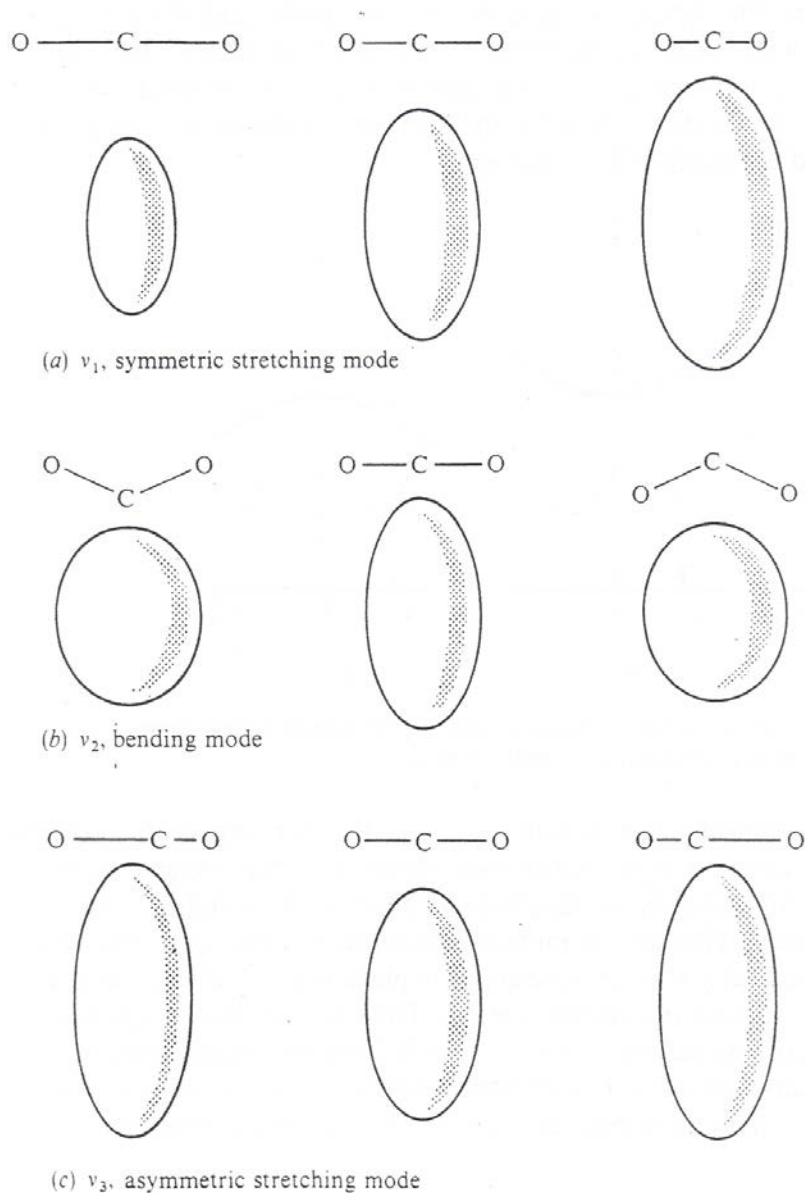
The shape of the polarizability el1ipsoid of the carbon dioxide molecule during its vibrations.

To do this it is usual to discuss the change of polarizability with some *displacement coordinate,* normally given the symbol ξ; contract. Thus we can sketch the variation of α with ξ as in the figure below with *small* displacements;.

(a) v_1 (b) v_2 (c) v_3
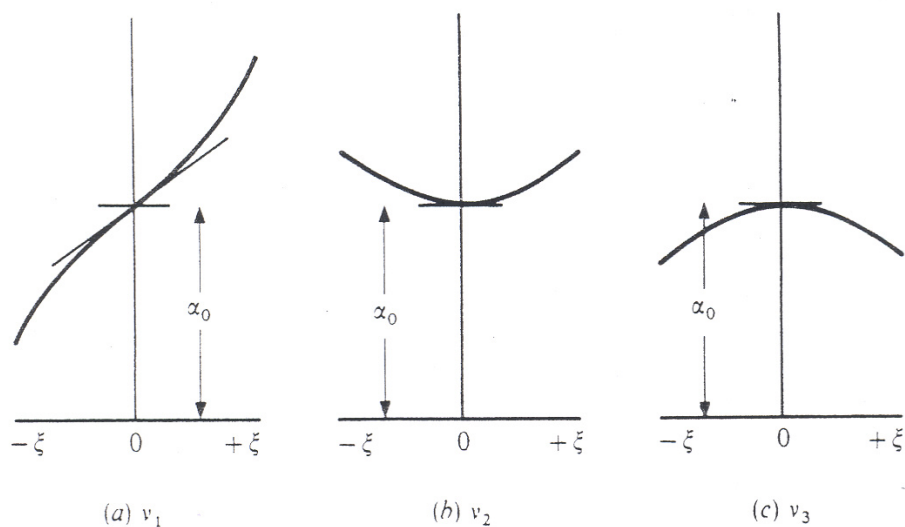
The variation of the polarizability, α, with the displacement coordinate, ξ, during the three vibrational modes of the carbon dioxide molecule.
**Raman and infrared activities of carbon dioxide**

Mode of vibration of CO_2	Raman	Infrared
v_1 : symmetric stretch	Active	Inactive
v_2 : bend	Inactive	Active
v_3 : asymmetric stretch	Inactive	Active

Rule of mutual exclusion. If a molecule has a *centre of symmetry* then Raman active vibrations are infrared inactive, and vice versa. If there is no centre of symmetry then some (but not necessarily all) vibrations may be both Raman and infrared active.
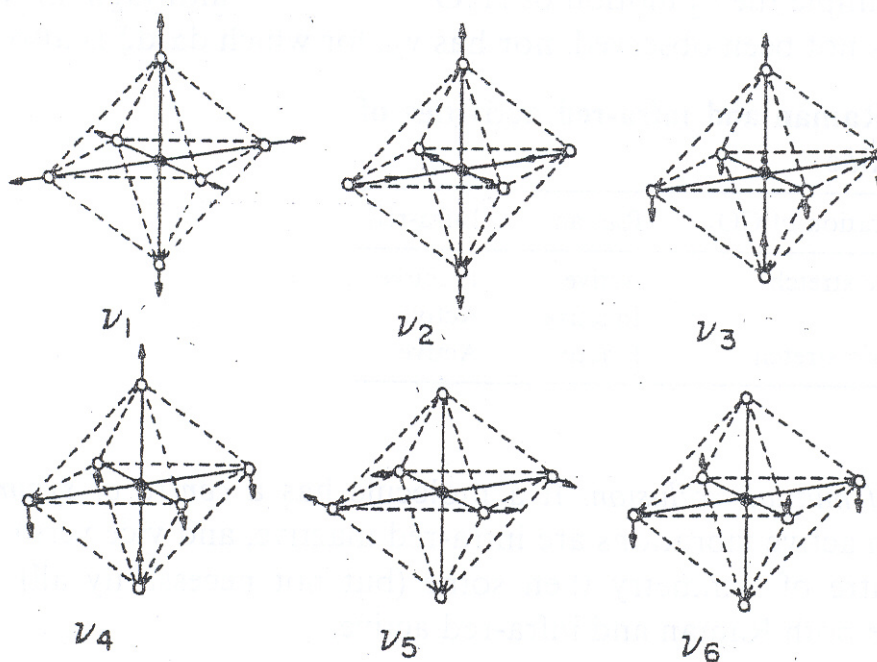
Examples

Which vibrations are active in Raman, which are active in IR and which are polarized or depolarized?
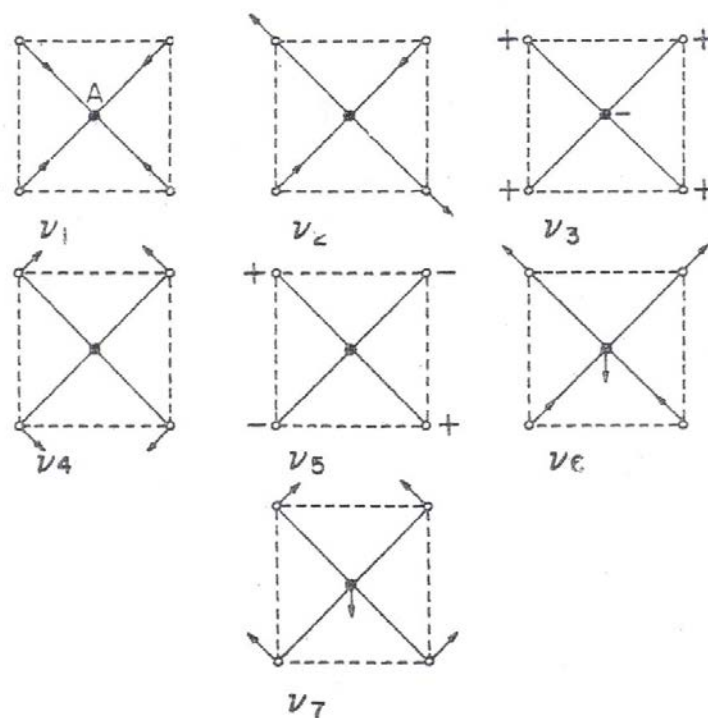
1. Acetylene
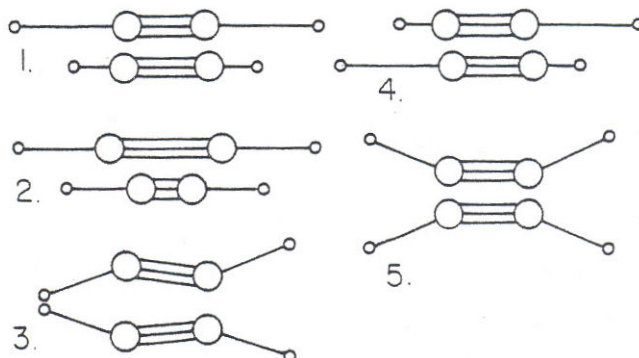
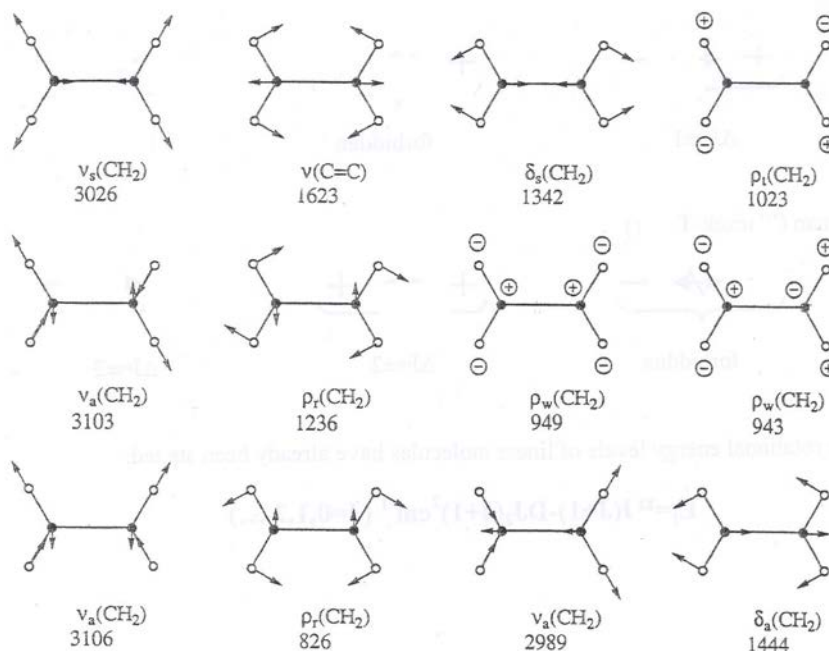**The vibrations of acetylene, H – C ≡ C – H.**

2. Octahedral molecules

Normal modes of vibrations of octahedral AB₆ molecule-point group O_h.

3. Square planar molecules

Normal modes of vibrations of square planar AB, molecule-point group D_{4h}

4. Ethylene

Approximate normal modes of vibration of ethylene. Symmetry, vibrational assignments, and observed frequencies (cm^{-1}) are given for each vibration. The $v(C=C)$ and $\delta_s(CH_2)$ are vibrationally coupled in the A_g species.

Selection rules: contrasting IR and Raman spectra

The common observations about Raman spectral intensities in four main generalizations:

- Stretching vibrations associated with chemical bonds should be more intense than deformation vibrations.
- Multiple chemical bonds should give rise to intense stretching modes, e.g., a Raman band due to a C=C vibration should be more intense that that due to a C-C vibration.
- Bonds involving atoms of large atomic masses are expected to give rise to stretching vibrations of high Raman intensity. The S-S linkages in proteins are good examples of this.
- Those Raman features arising from normal coordinates involving two in-phase bond stretching motions are more intense than those involving a 180° phase difference. Similarly, for cyclic compounds the in-phase "breathing" mode is usually the most intense.

Table 1.1 Characteristic Wavenumbers and Raman and Infrared Intensities of Groups in Organic Compounds

Vibration[a]	Region(cm^{-1})	Intensity[b] Raman	Infrared
ν(O-H)	3650-3000	w	s
ν(N-H)	3500-3300	m	m
$\nu(\equiv$C-H)	3300	w	s
ν(=C-H)	3100-3000	s	m
ν(-C-H)	3000-2800	s	s
ν(-S-H)	2600-2550	s	w
ν(C$\equiv$N)	2255-2220	m-s	s-0
ν(C$\equiv$C)	2250-2100	vs	w-0
ν(C=O)	1820-1680	s-w	vs
ν(C=C)	1900-1500	vs-m	0-w
ν(C=N)	1680-1610	s	m
ν(N=N), aliphatic substituent	1580-1550	m	0
ν(N=N), aromatic substituent	1440-1410	m	0
ν_a((C-)NO$_2$)	1590-1530	m	s
ν_s((C-)NO$_2$)	1380-1340	vs	m
ν_a((C-)SO$_2$(-C))	1350-1310	w-0	s
ν_s((C-)SO$_2$(-C))	1160-1120	s	s
ν((C-)SO(-C))	1070-1020	m	s
ν(C=S)	1250-1000	s	w
δ(CH$_2$), δ_a(CH$_3$)	1470-1400	m	m
δ_s(CH$_3$)	1380	m-w, s, if at C=C	s-m

ν(CC), aromatics	1600, 1580	s-m	m-s
	1500, 1450	m-w	m-s
	1000	s (in mono-; m-; 1,3,5-derivatives)	0-w
ν(CC), alicyclics, and aliphatic chains	1300-600	s-m	m-w
ν_a(C-O-C)	1150-1060	w	s
ν_s(C-O-C)	970-800	s-m	w-0
ν_a(Si-O-Si)	1110-1000	w-0	vs
ν_s(Si-O-Si)	550-450	vs	w-0
ν(O-O)	900-845	s	0-w
ν(S-S)	550-430	s	0-w
ν(Se-Se)	330-290	s	0-w
ν(C(aromatic)-S)	1100-1080	s	s-m
ν(C(aliphatic)-S)	790-630	s	s-m
ν(C-Cl)	800-550	s	s
ν(C-Br)	700-500	s	s
ν(C-I)	660-480	s	s
δs(CC), aliphatic chains	400-250	s-m	w-0
C_n, n = 3,...,12			
n> 12	2495/n		
Lattice vibrations in molecular crystals (liberations and translational vibrations)	200-20	vs-0	s-0

[a]ν, stretching vibration; δ, bending vibration; ν_s, symmetric vibration; ν_a, antisymmetric vibration.

[b]vs, very strong; s, strong; m, medium; w, weak; 0, very weak or inactive.

RAMAN VERSUS INFRARED SPECTROSCOPY

RAMAN		IR
	Selection rules	
active	(mutual exclusion)	active
	Intensities	
Strong in Raman: $C\equiv C$, $C=C$, $P=S$, $S\text{-}S$, etc.		Strong in IR $O\text{-}H$, $N\text{-}H$, $C=O$, etc.
	Depolarization ratios (ρ)	
Only in Raman		Not in IR
	Enhancements	
Resonance Raman SERS, SERRS, SMS, (biology)		Not in IR SEIRA (?)
	Samples size	
Less then 1 mm		Difficult in IR
	Aqueous solutions	
H_2O is a bad scatter (biology)		H_2O is a strong absorber
	Sample holders	
Sealed glass tubs		Glass is not possible
	Spectral range	
$4000\text{-}50\ cm^{-1}$ is covered		$4000\text{-}50\ cm^{-1}$ need MIR and FIR spectrometers
	Sources	
Leaser can cause heating effects.		No real heating effect.
	Electronic excitations	
Fluorescence		Not effected
	Rotational fine structure	
Difficult to resolve (UV, VIS region)		High resolution: easier to realize.
	Instrument expenses	
Research Raman is Expensive		Research IR is cheaper
Difficult	**Gas spectra**	Easy

Comparison of basic applications

	Raman	Infrared
Fingerprinting	Excellent	Excellent
Best vibrations	Symmetric	Asymmetric
Assignment work	Excellent	Very good
Group frequencies	Excellent	Excellent
Aqueous solutions	Very good	Very difficult
Quantitative analysis	More difficult	Good
Low frequency modes	Excellent	Difficult

Examples for structural determination

Infrared ad Raman spectra of nitrous oxide

$\bar{v}$ (cm⁻¹)	Infrared	Raman
589	Strong	-
1285	Very strong	Very strong; polarized
2224	Very strong	Strong; polarized

What is the structure:

a, N=O=N   linear

b, N⌒O⌒N   bend

c, N-N-O   linear

Infrared and Raman spectra of NO_3^- and ClO_3^-

Nitrate ion (NO_3^-)			Chlorate ion (ClO_3^-)		
Raman (cm⁻¹)	Infrared (cm⁻¹)	Assignment	Raman (cm⁻¹)	Infrared (cm⁻¹)	Assignment
690 *dp*	680 ⊥	v_4	450 (depol.)	434 ⊥	v_4
-	830 ∥	v_2	610 (pol.)	624 ∥	v_2
1049 *p*	-	v_1	940 (depol.)	950 ⊥	v_3
1355 *dp*	1350 ⊥	v_3	982 (pol.)	994 ∥	v_1

Which molecule is planar and which is pyramidal?

$v_1(A'_1)$
$v_s(XY)$

$v_2(A''_2)$
$\pi(XY_3)$

$v_3(E')$
$v_a(XY)$

$v_4(E')$
$\delta_d(YXY)$

$v_1(A_1)$
$v_s(XY)$

$v_2(A_1)$
$\delta_s(YXY)$

$v_{3a}(E)$
$v_d(XY)$

$v_{4a}(E)$
$\delta_d(YXY)$
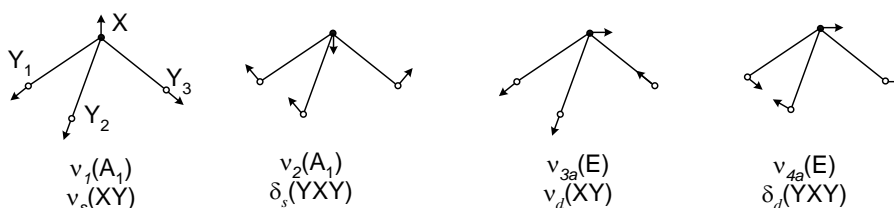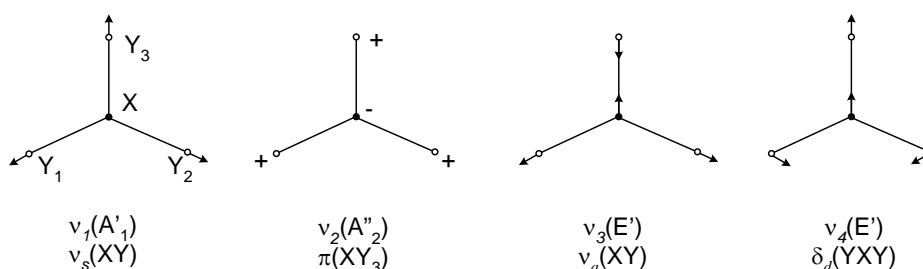
INFRARED AND RAMAN SPECTRA OF TWO METAL TETRACHLORIDES

	$MC1_4$		$MC1_4$	
	Raman	IR	Raman	IR
ν_1	369 s, p	-	303 s, p	-
ν_2	95 w, dp	-	168 w, dp	-
ν_3	408 w, dp	407 s	-	150w
ν_4	126 m, dp	176w	175 m, dp	-
ν_5	-	-	-	321 S
ν_6	-	-	-	161 w, b

Possible structures:

a, Square planar?
b, Pyramida1?
c, Tetrahedral?

Lasers for Raman spectroscopy

Dispersive systems: 488, 514.5, 532, 632.8, and 785 nm
FT-Raman: 1064 nm

CW Lasers for Analytical Raman Spectroscopy

Type	λ(nm[a])	Power (typical)	Comments
Doubled Ar$^+$	244, 257, 229	15-200 mW	*b,c,d*
Ar$^+$ (air cooled)	488.0, 514.5	5-50 m W	
Ar$^+$ (water cooled)	351.1	0.1-10 W	*b,c,d*
	457.9		
	476.5		
	488.0		
	496.5		
	514.5		
	528.7		
He-Ne	632.8	5-100 mW	
Kr$^+$	413.1	0.1-4 W	*b,c,d*
	647.1		
	752.5		
Nd:YAG	1064	0.1-10 W	*e*
Doubled Nd: YAG	532	0.05-5 W	*e*
Diode	670-865 nm	0.01-1 W	*f*

[a]Commonly available output wavelengths. Others available as noted in Table 7.2.
[b]Requires water cooling.
[c]Requires 208 or 480 V power.
[d]Tunable to one of indicated lines.
[e]*Some* versions require water cooling and/or 208 V power.
[f]Continuously tunable wavelength within limited range.

Remarks:

- CW continuous wave, not pulsed;

- frequency stability $< 1\text{cm}^{-1}$ (No line broadening)

- output line width $100\text{-}10^{-4}$ cm^{-1} (variable)

$$1\text{cm}^{-1} = 30 \text{ GHz}, \ 10.4 \text{ cm}^{-1} = 1 \text{ MHz}$$

- gas lasers (Ar$^+$, Kr$^+$, He-Ne, He-Cd)

- solid state lasers (luminescence)
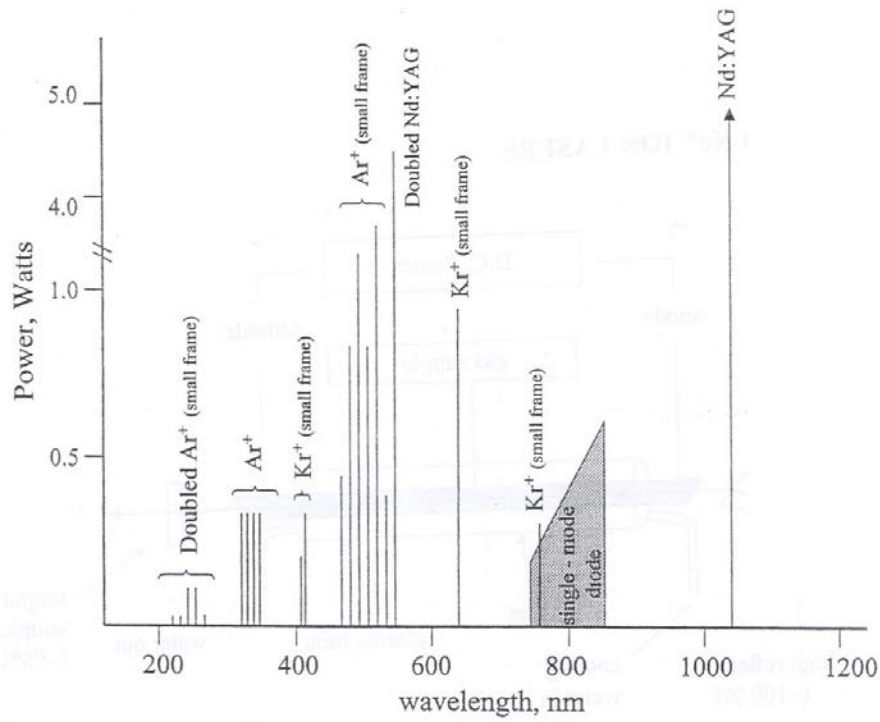
Wavelengths and available power ranges of commercial lasers commonly used for Raman spectroscopy. Note discontinuity in power axis above 1 W. Diode lasers are available over a range of wavelengths and are to some extent tunable.

Ar$^+$ and Kr$^+$ ion lasers
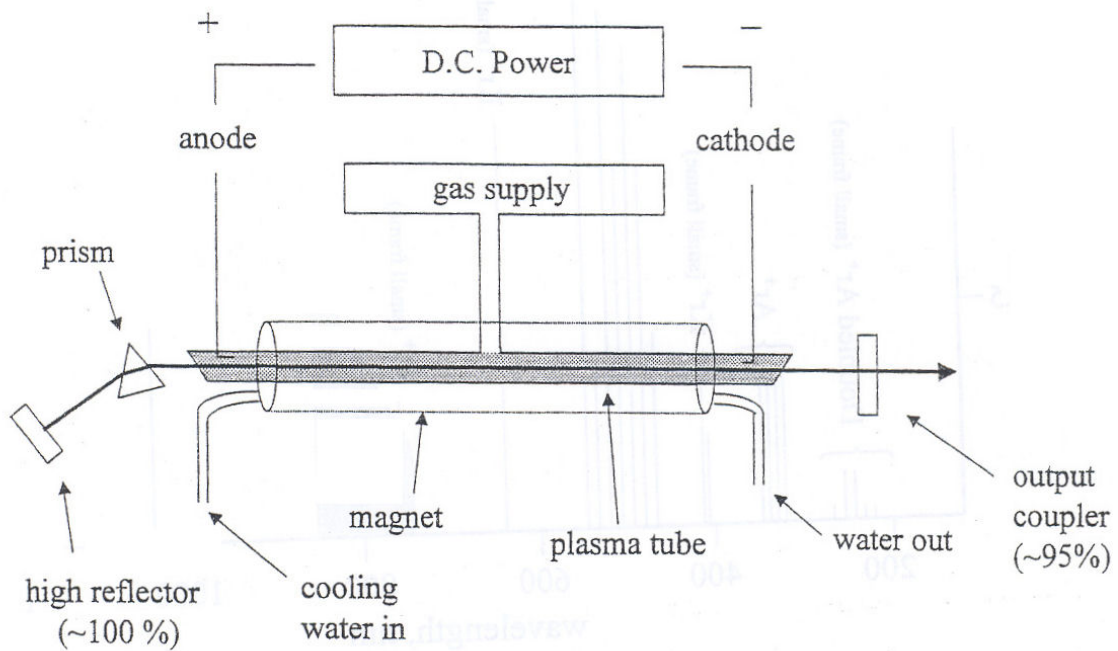
Schematic of argon ion laser, including a cylindrical magnet to confine the plasma.

Large laser implies:

- 480W, three-phase 60kW

- intensive water cooling

- 0.01-0.05% of the electrical energy is converted to laser light.

Expensive (50.000 USD, Tube: 15.000 USD)

Air coaled small *Ar$^+$* lasers are cheaper.

Ultraviolet Ion Lasers

Ultraviolet output is available from both Ar^+ and Kr^+ lasers, sometimes with relatively minor modification. For a conventional large-frame Ar^+ laser, the mirrors may be changed to optimize UV performance.

Ultraviolet Wavelengths and Powers. (W) of Ion Lasers

Wavelength (nm)	Ar^{+a}	Kr^{+a}	Doubled Ar^{+b}
351.6-385.8*	3.0		
333.6-363.8*	5.0		
337.5-356.4*		2.0	
245.4-305.5*	0.60		
264			0.02^b $(0.10)^a$
257			0.02 $(1.0)^a$
248			0.03 $(0.30)^a$
244			0.10 $(0.50)^a$
238			0.03 $(0.10)^a$
229			0.01 $(0.04)^a$

[a]Large frame

[b]Small frame

*Closely spaced lines

The v_0^4 effect:

λ (nm)	v_0 (cm^{-1})	Raman efficiency $(v_0)^4$
1064	9398.5	44
785	12738.8	149
632.8	15802.8	354
514.5	19436.3	809
488.0	20491.8	1000
413.1 (Kr^+)	24207.2	1947
351.1	28481.9	3732
264	37878.8	11675
244	40983.6	16000
229	43998.1	20622

HELIUM-NEON LASERS

Properties:

- Frequency accuracy is excellent (Ne atom emission)
- Long life
- Low cost, but low power (0.5-100 m W)
- The silicon CCDs are most sensitive in red region

NEODYMIUM-YAG (Nd:YAG)

Nd:YAG lasers differ fundamentally from He-Ne and ion lasers in that the lasing medium is a solid rather than a gas. The density of excited states can be much higher, and the gain medium much smaller. YAG is yttrium aluminium garnet ($Y_3Al_5O_{12}$), usually in the shape of a rod a few millimetres in diameter and few centimetres in length. The YAG is a host to Nd^{3+} ions, which are actually the lasing medium. YAG has more attractive optical and heat transfer properties than the glass used in large, pulsed Nd:glass lasers. The Nd:YAG is a "four-level" laser and is much more efficient than its historical predecessor, the three-level ruby laser based on Cr^{3+} in an Al_2O_3 host
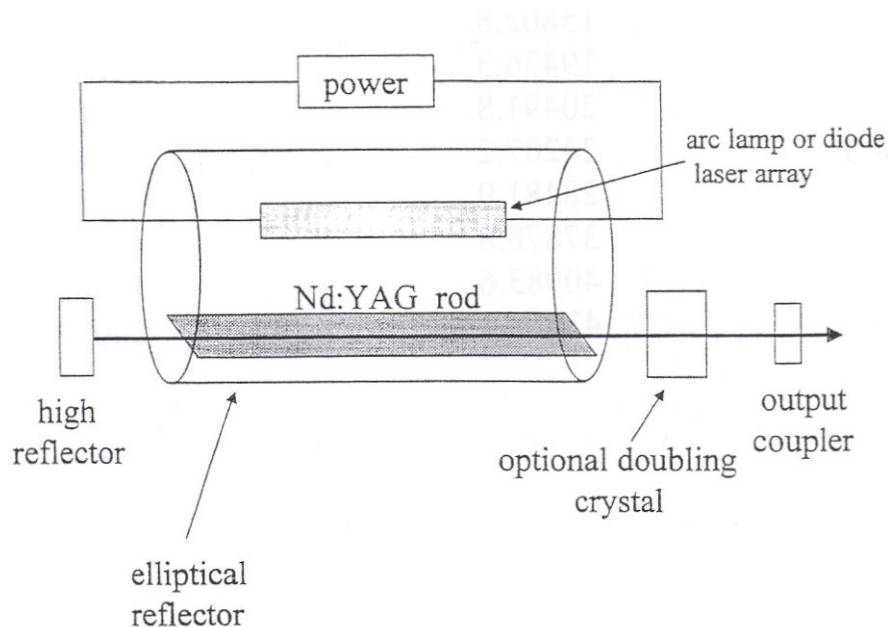
Schematic of Nd:YAG laser, pumped by an arc lamp or diode laser array. Doubling crystal converts 1064 nm light to 532 nm

ISOTOPE EFFECT IN CCl$_4$ (resolution check)

The ν_1 vibration of CC1$_4$ of 459 cm^{-1} with a good resolution appears with distinct multiple structures show or below:

$\Delta\nu$ cm-1
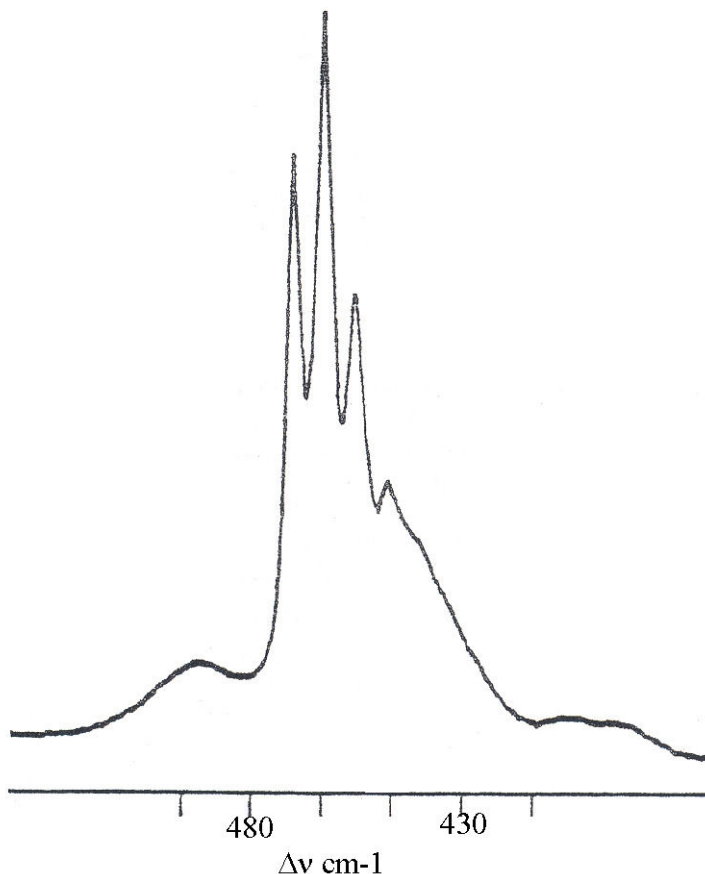
Chlorine Isotope Bands

Isotopic modifications	Percentage	Experimental frequency (cm^{-1})	Calculated frequency (cm^{-1})
C^{37}Cl$_4$	0.4	-*	449.7
C^{35}Cl^{37}Cl$_3$	7.4	452.0	452.8
C^{35}Cl$_2^{37}$Cl$_2$	21.1	456.4	455.9
C^{35}Cl$_3^{37}$Cl	42.2	459.4	459.2
C^{35}Cl$_4$	31.6	462.4	462.4

*Not observed

Detectors for Raman spectroscopy

Specificity: small signal

                    sensitive det.

                    Low noise det.

PM-tubes (~1960), photon counting (~1970) CCD (~1985)

MULTI CHANNEL DETECTION

Photons in the 200 to 1100 nm range, generate photoelectrons, Q is the probability of generating a photoelectron.
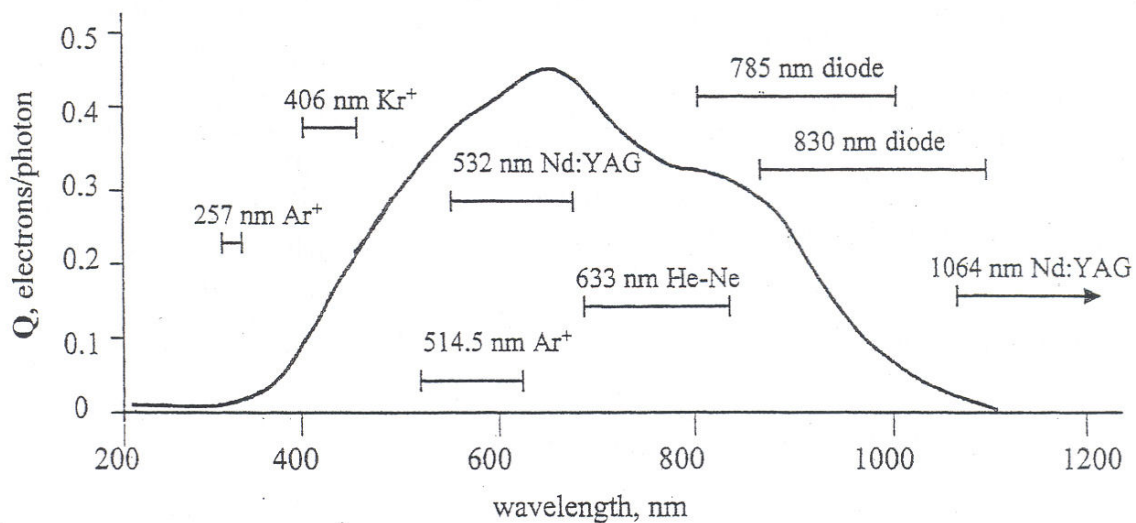
Typical of Q vs. λ curve for a front-illuminated silicon CCD, with Raman shift ranges (0 to 3000 cm^{-1}) for several common lasers.
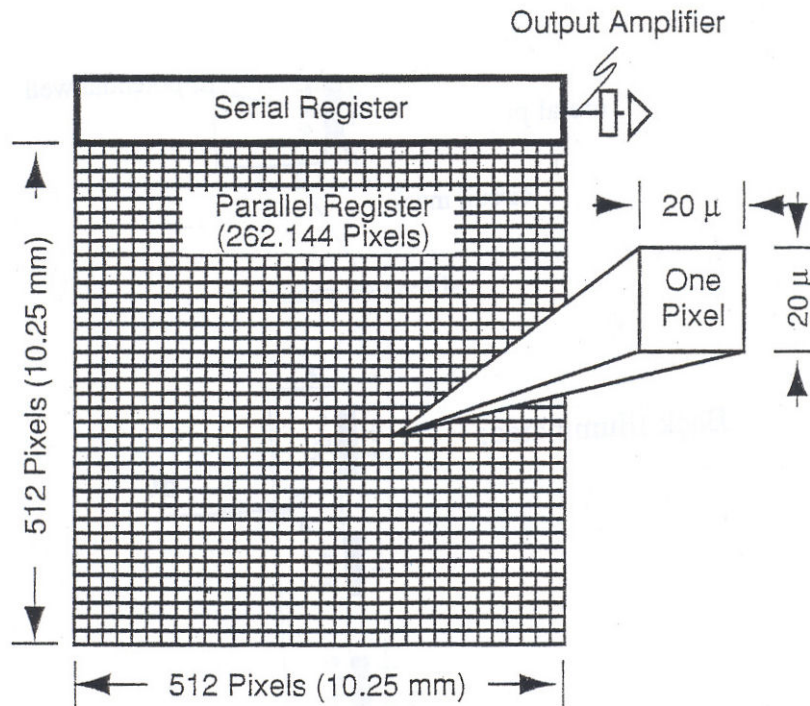
Schematic of a CCD detector

Advantages:

- Low readout noise
- High quantum efficiency (85-95%) and sensitivity - width broad wavelength range (120-1000nm)
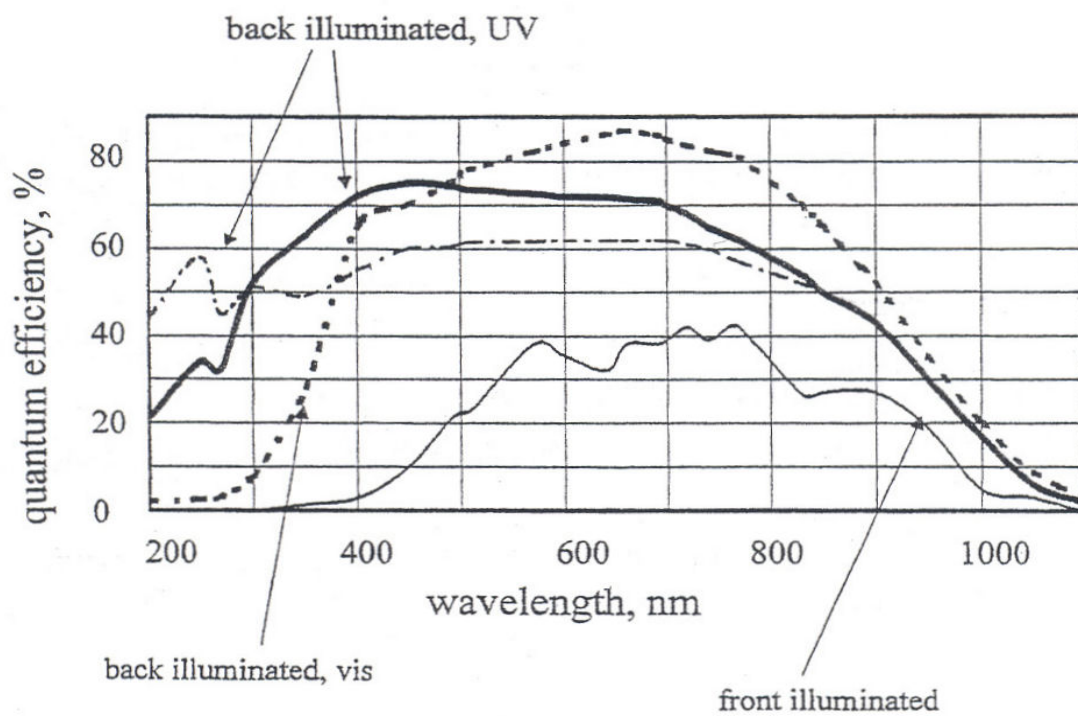
Quantum efficiency curves for several CCD types
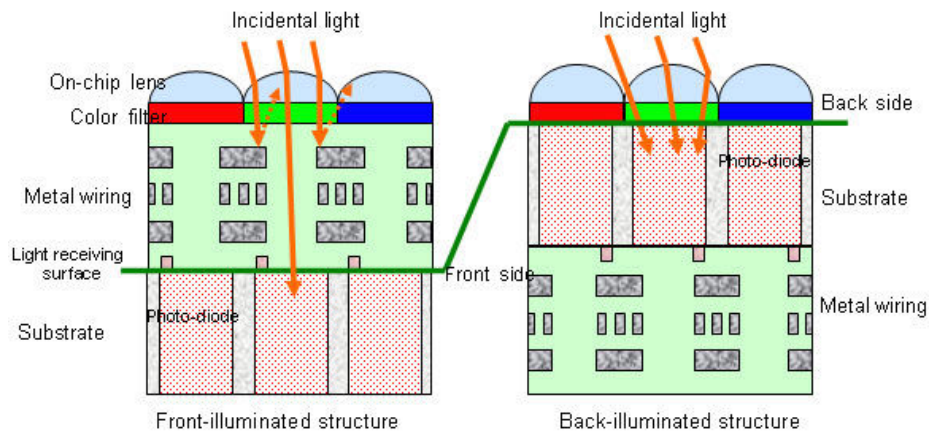
Front- (left) and Back-illuminated CCD detectors

FT-Raman Detectors
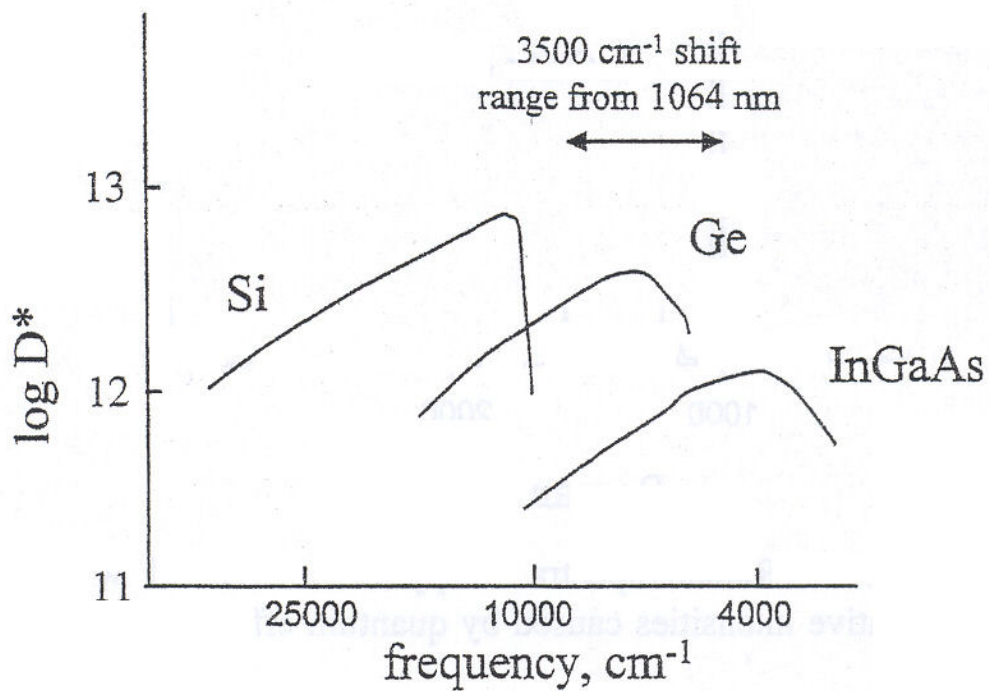
Response curves of semiconductor detectors, with Raman shift range shown relative to 1064 nm. $D*$ is proportional to quantum efficiency and is defined in the FTIR literature.

- The curves are temperature dependent
- Response vary with Cu doping in Ge

3.1 DISPERSIVE SINGLE DETECTOR SYSTEMS

Major components:
(l) Excitation sources (lasers)
(2) Detectors
(3) Monochromators
(4) Sample illumination and collecting systems

Monochromators
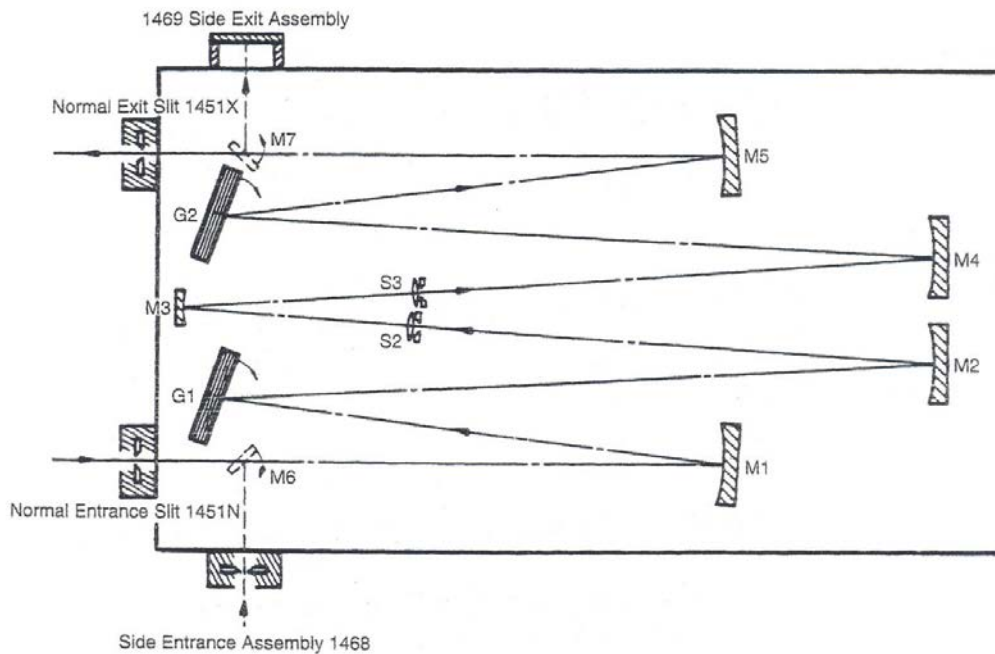
Schematic of a Spex Model 1403/4 double monochromator

Using an 1,800 grooves/mm grating, the double monochromator being discussed can cover the range from 31,000 to 11,000 cm^{-1} .

Triple Spectrographs

Single monochromator: insufficient stray light

Double monochromator: reduces stray light (10^{-10})

Triple spectrograph:

- variable excitation is possible

- low frequency range (10-20 cm^{-1})

- Stray light $<10^{-12}$
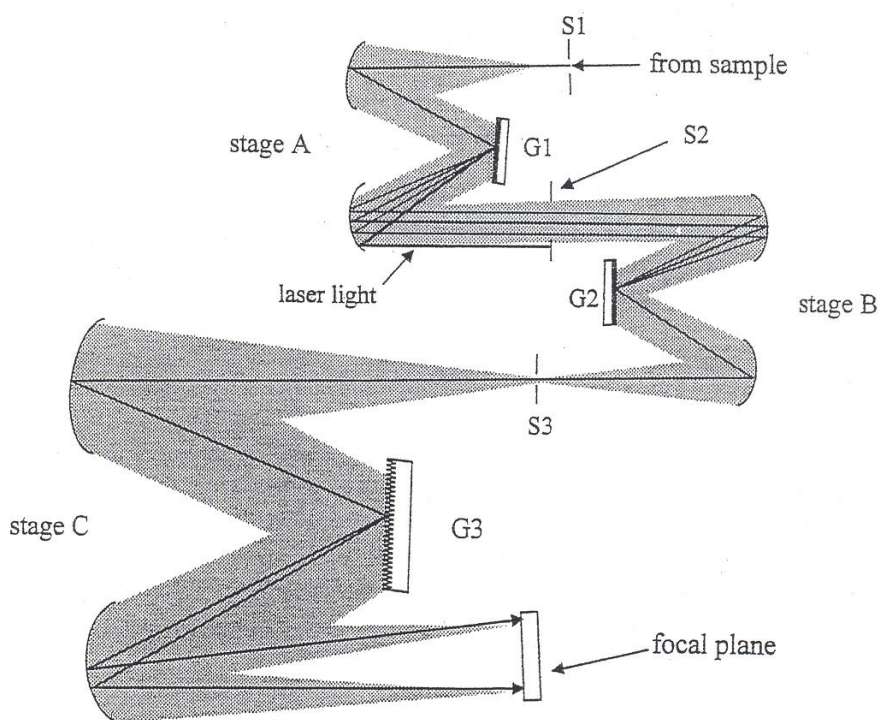
Schematic of a triple spectrograph, consisting of a subtractive dispersion double monochromator preceding a single spectrograph. Similar to Spex "Triplemate" or Dilor "X-Y."
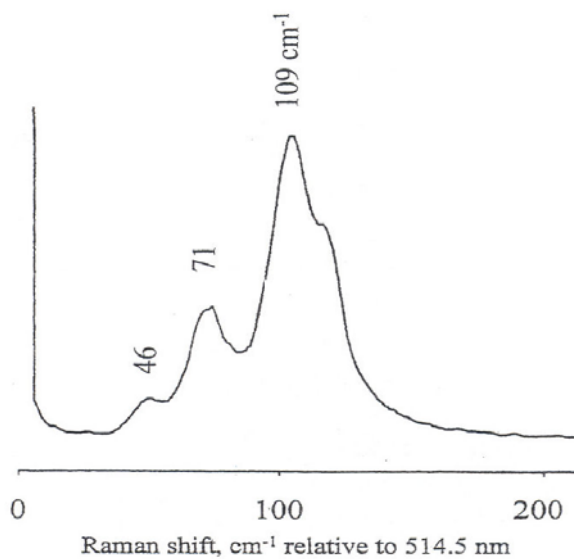
Low Raman shift bands of solid naphthalene
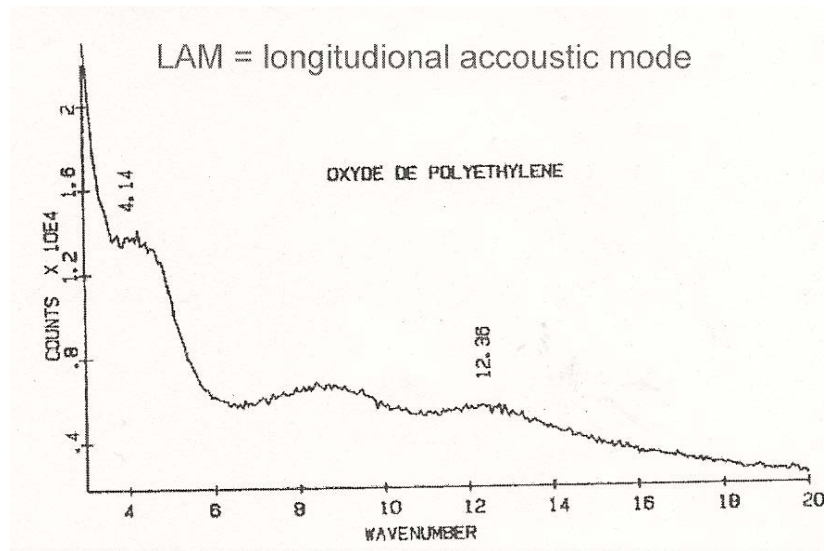
Low frequency acoustic modes of polyethylene oxide

Holographic Grating Spectrographs

Available: from 1990s

- 2 glass/ quartz plates, between photoactive emulsion
- exposed by interference pattern, that generate holographic image in the emulsion
- used in transmission mode
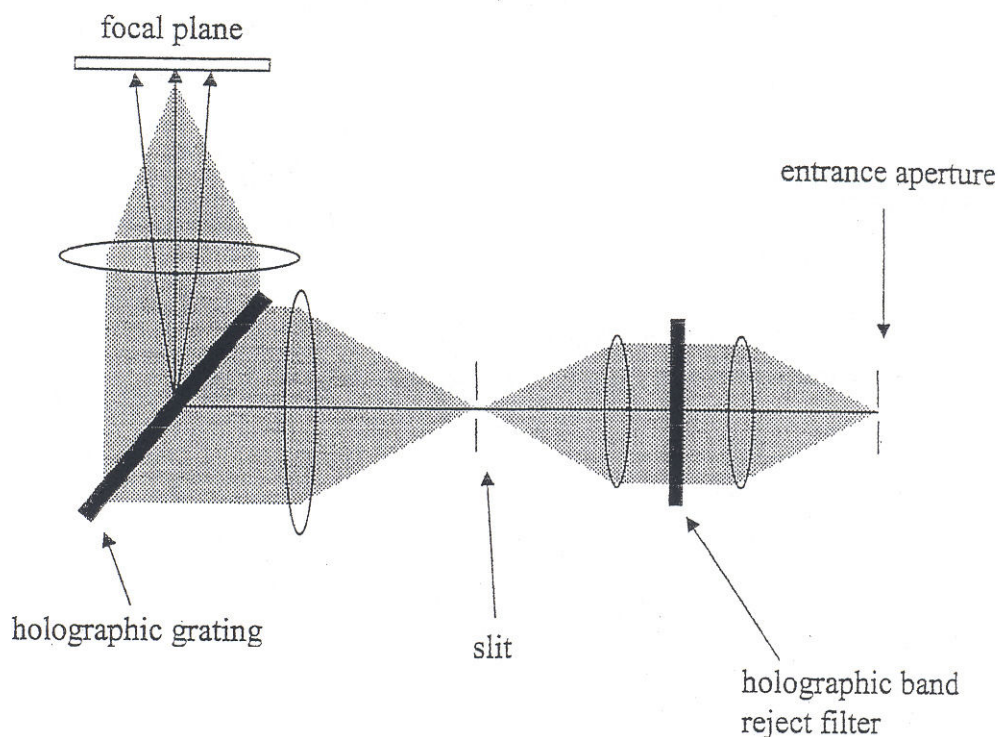
Schematic of axial transmission holographic spectrograph

Advantages:
1) Optical axes are perpendicular to lenses, less aberration, better image quality,
2) High transmission,
3) Very low f/# (1.5 - 1.8) is possible,
4) Image is in good compatibility with CCD detectors.

Disadvantages:
1) Good for illumination only with one laser,
2) Emulsion - not allows to work in UV region.

3.2. MULTICHANNEL DISPERSIVE SPECTROMETERS

Multichannel visible detectors: Photodiodes 1970s (~500 elements)

No exit slit

Each detector elements detect different colours
Resolution: depends on the number of detectors elements
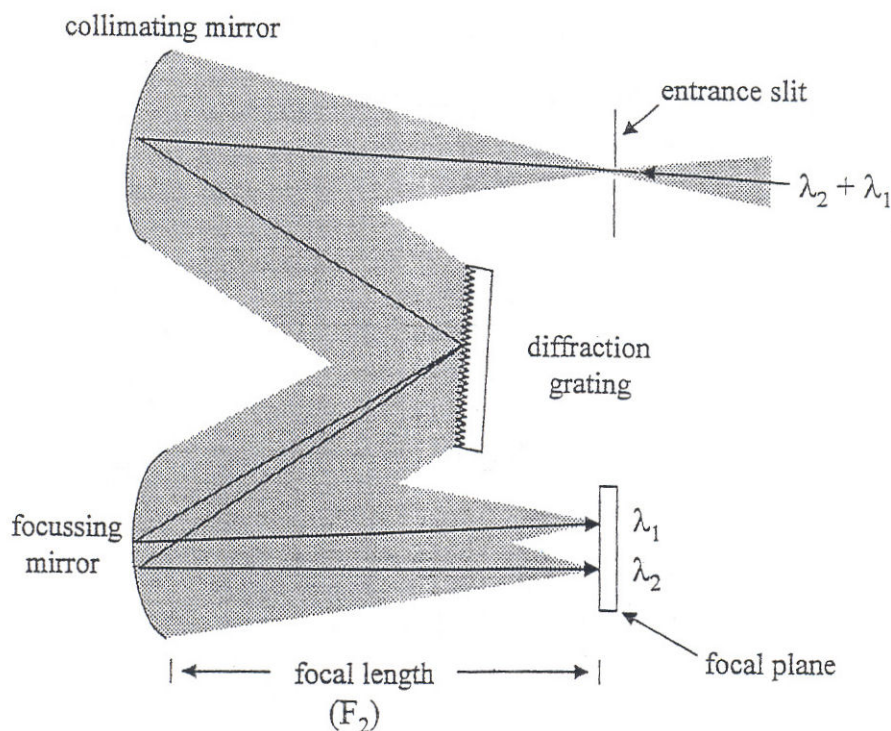Photon gains: 10^3 - 10^4 (Si photodiodes)
CCD is available since1980s
Efficiency very high (0.99999), 600 x 300, 1000 x 300 pixels
CCD is a **two dimensional** array, whereas diode arrays were strictly linear arrays

Advantages:
1) Raman **imaging** in real time, microscopy
2) Pixels in **vertical** columns can be **co added,** $\rightarrow$ speed $\rightarrow$ sensitivity, $\left(\sqrt{N_D}\right)$

Schematic of a single grating Czerny- Turner spectrograph. Shading indicates envelope of light passing through the instrument. This disperses and focuses wavelengths at the focal-plane.
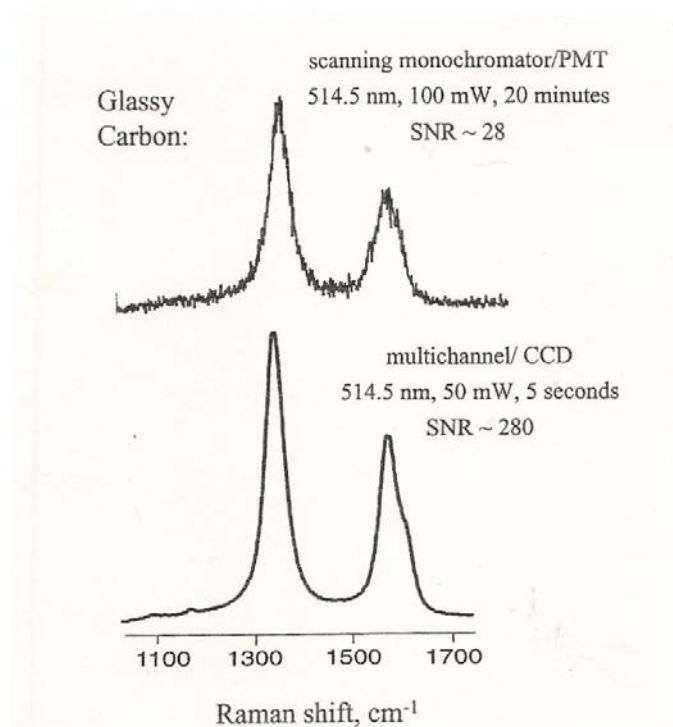
Raman spectra of Glassy Carbon recorded with single-channel and multi-channel spectrometers (N_d=512)

SNR= Signal Noise Ratio can be calculated as:
SNR(multi)/SND(single) = $(N_d)^{1/2}$ = $(512)^{1/2}$ ~ 23 (Multichannel Advantage)

General view of Horiba Scientific LabRAM HR *Evolution* Raman microscope spectrometer (SU), u_0= 532, 633, 785nm

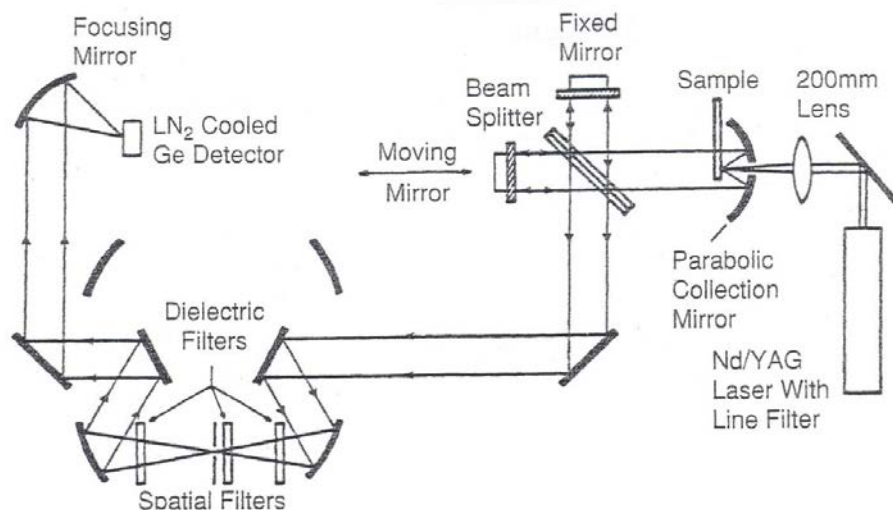**The fantastic Renishaw Raman microscope in TUM CRC, υ_0=266, 532, 633, 785nm**

3.3. FOURIER TRANSFORM RAMAN

SPECTROMETERS

Late development (1982), why:
- The ν_0^4 – factor in long wavelengths;
- More precise interferometers (in 0.7 - 1.2 μm range)
- Shorter sampling distances (λ/4, λ /8 He-Ne)
- Lack of lasers in NIR

**Raman spectrometer (B. Chase) based on Digilab FTS-20 interferometer.**

Advantages and Disadvantages of FT-Raman

Advantages	Disadvantages
Reduction or elimination of fluorescence	Absorptions in the NIR
High resolution	Black-body emissions in IR
High throughput	Lower scattering intensity due to v^4
Good frequency accuracy	effect
Collect Stokes and anti-Stokes	Difficult to detect low
Raman simultaneously	concentrations of impurities
Both IR and Raman capabilities on same instrument.	
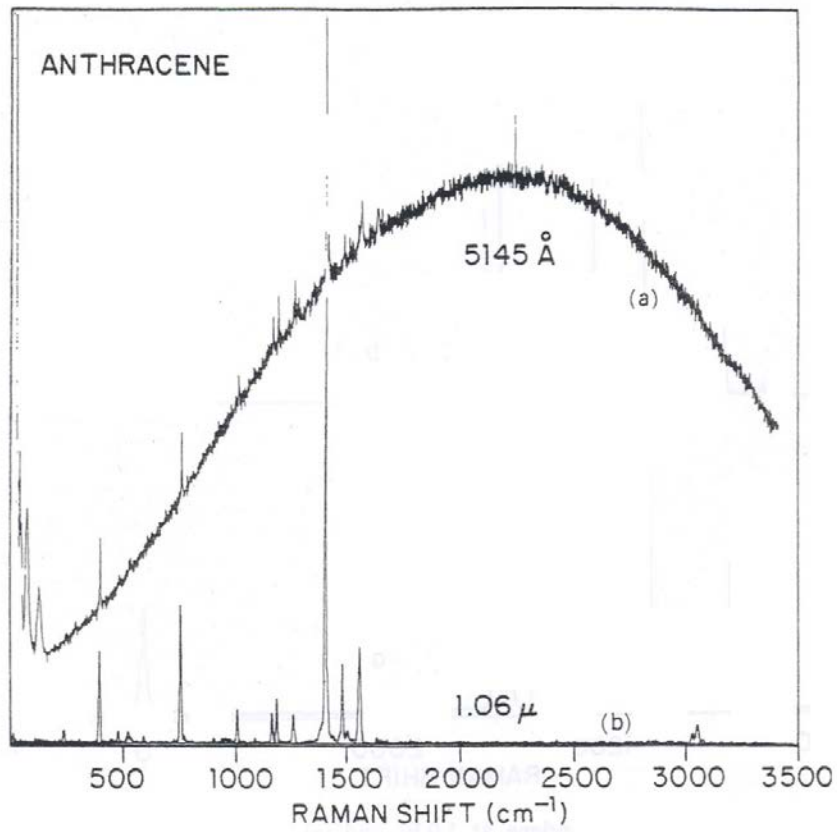
(a) Raman spectrum of anthracene at 514.5-nm excitation. (b) FT-Raman spectrum of anthracene at 1.06-μm excitation.

(
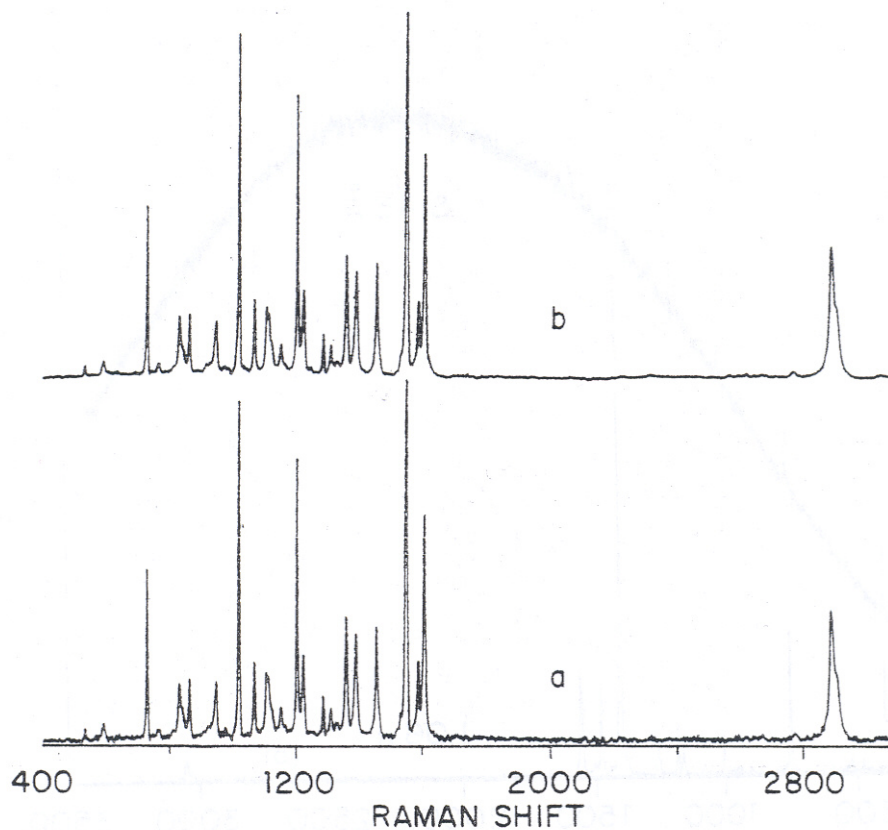
FT-Raman spectrum of indene at 1.0 W and (a) 2-s and (b) 30-s measurement time

Examples of FT -Raman Applications

Application	Comments	Reference
Lipids, solvents	Fiber-optic sampling	16
Pure solids, liquids	Fiber-optic sampling	22
Polyethylene, PET		17
Cimetidine polymorphs		18
Fluorescent samples	Pulsed, step-scan	19
Adsorbed monolayers	Surface-enhanced FT-Raman	30-32
Biological macromolecules		33
Food analysis	Carotenoid, fatty acids	34
Sugars, proteins	2-D correlation with NIR absorption	35
Oxygenates in gasoline	Compared to NIR	36
Petroleum additives	Compared to mid-IR and NIR	37
Low-density polyethylene	Multivariate data analysis	38
Oxygenates in gasoline	Compared to FT-IR, NIR	39
Basal cell carcinoma	Diagnostic	40
High-temperature polymerization	>250°C	41

DEDICATED FT-RAMAN SYSTEM (HAS, Budapest), $u_0=1064$ nm

REFERENCES

1. D. B. Chase, J. F. Rabolt, *Fourier Transform Raman Spectroscopy: From Concept to Experiment,* Academic Press, New York, 1994.

2. D. B. Chase, *Anal. Chem.* **59**; 881A (1987).

3. P. Hendra, C. Jones, and G. Warnes, *FT-Raman: Instrumentation and Chemical Application,* Ellis Harwood, New York, 1991.

4. P. Hendra; in J. J. Lasema, ed., *Modem Techniques in Raman Spectroscopy,* Wiley, London, 1996.

5. M. Schaeberle, H. Morrison, J. Turner III, and P. 1. Treado, *Anal. Chem.,* **71**, *175A* (1999).

6. D. N. Batchelder, C. Cheng, and G. D. Pitt, *Adv. Mater.,* **3**, 565 (1991).

7. Datex/Ohmeda, Inc., Madison, Wisconsin.

8. G.I. Puppels, M. Grond, and J. Greve, *Appl. Spectrosc.,* **47**, 1256 (1993).

9. E. N. Lewis, P. J. Treado, and I. W. Levin, *Appl. Spectrosc.,* **47**, 539 (1993).

10. M. Schaeberle, V. F. Kalasinsky, J. L. Luke, E. N. Lewis, I. W. Levin, and P. J. Treado, *Anal. Chem.,* **68**, 1828 (1996).

11. J. P. Ingle and S. R. Crouch, *Spectrochemical Analysis,* Prentice-Hall, Englewood Cliffs, NJ, 1988, P 61.

12. K. Christensen, N. Bradley, M. D. Morris, and R. V. Morrison, *Appl. Spectrosc.,* **49**, 1120 (1995).

13. ChemIcon Inc., 7301 Penn Avenue, Pittsburgh, PA 15208.

14. C. J. Petty, G. M. Warnes, P. J. Hendra, and M. Judkins, *Spect. Acta,* **47A**, 1179 (1991).

15. D. B. Chase and B. A. Parkinson, *Appl. Spectrosc.,* **42**, 1186 (1988).

16. N. Lewis, V; F. Ka1asinsky, and 1. W. Levin, *Anal. Chem.,* **60**, 2658 (1988).

17. B. Schrader, A. Hoffman, A. Simon, and J. Sawatzki, *Vibrational Spec.,* **1**, 239 (1991).

18. B. Schrader, A. Hoffman, and S. Keller, *Spect. Acta,* **47A** 1135 (1991).

19. J. P. Insle and S. R. Crouch, *Spectrochemical Analysis;* Prentice-Hall, Englewood Cliffs, NJ, 1988, p. 81.

20. J. P. Insle and S. R. Crouch, *Spectrochemical Analysis;* Prentice-Hall, Englewood C1iffs, NJ, 1988, p. 83.

21. P. Jaako1a, J. D. Tate, M. Paakunainen, J. Kauppinen, and P. Sirenian, *Appl. Spectrosc.,* **51**, 1159 (1997).

22. D. D. Archibald, L. T. Lin, and D. E. Honigs, *Appl. Spectrosc.,* **42**, 1558 (1988).

23. J. Zhao and R. L. McCreery, *Appl. Spectrosc.,* **50**, 1209 (1996).

24. J. Zhao and R. L. McCreery, *Appl. Spectrosc.,* **51**, 1687 (1997).

25. K. J. Asselin and B. Chase, *Appl. Spectrosc.,* **48**, 699 (1994).

26. B. Chase and Y. Talmi, *Appl. Spectrosc.,* **45**, 929 (1991).

27. B. A. Barrera and A. J. Sommer, *Appl. Spectrosc.,* **52**, 183 (1998).

28. G. Jalsovsky, O. Egyed, S. Holly, and B. Hegedus, *Appl. Spectrosc.,* **49**, 1142 (1995).

29. A. Sakamoto, Y. Furukawa, M. Tasumi, and K. Masutani, *Appl. Spectrosc.,* **47**, 1457 (1993).

30. S. M. Angel, L. F. Katz, D. D. Archibald, L. T. Lin, and D. E. Honigs, *Appl. Spectrosc.,* **42**, 1327 (1988).

31. S. M. Angel, L. F. Katz, D. D. Archibald, and D. E. Honigs, *Appl. Spectrosc.,* **43**, 367 (1989).

32. S. M. Angel and D. D. Archibald, *Appl. Spectrosc.,* **43**, 1097 (1989).

33. E. N. Lewis, V. F. Kalasinsky, and I. W. Levin, *Appl. Spectrosc.,* **48**, 1188 (1988).

34. Y. Ozaki, R. Cho, K. Ikegaya, S. Muraishi, and K. Kawauchi, *Appl. Spectrosc.,* **46**; *1503* (1992).

35. W. F. McClure, H. Maeda, 1. Dong, Y. Liu, and Y. Ozaki, *Appl. Spectrosc.,* **50**, 467 (1996).

36. S. J. Choquette, S. N. Chesler, D. L. Duewer, S. Wang, and T. C. O'Haver, *Appl. Spectrosc.,* **68**, 3525 (1996).

37. J. B. Cooper, K. L. Wise, W. T. Welch, M. B. Sumner, B. K. Wilt, and R. R. Bledsoe, *Appl. Spectrosc.,* **51**, 1613 (1997).

38. K. Sano, M. Shimoyama, M.Ohgane, H. Higashiyama, M. Watari, M. Torno, T. Ninomiya, and Y. Ozaki, *Appl. Spectrosc.,* **53**, 551 (1999).

39. J. B. Cooper, K. L. Wise, W. T. Welch, R. R. Bledsoe, and M. B. Sumner, *Appl. Spectrosc.,* **50,** 917 (1996).

40. M. Gniadecka, H. C. Wulf, and N. N. Mortensen, *J. Raman Spec.,* **28**, 125 (1997).

41. J. F. Aust, J. B. Cooper, K. L. Wise, and B. J. Jensen, *Appl. Spectrosc.,* **53**, 682 (1999).

3.4. BASIC SAMPLING TECHNIQUES

Sampling overview

 The design and execution of the alignment between laser, sample, and collection aperture have a huge effect on the **magnitude and reproducibility** of the signal and the signal-to-noise ratio (**SNR).**
One must always keep in mind that Raman spectroscopy is a scattering technique with a generally **weak signal**, and the optical requirements are much more demanding than those of an absorption method such as Fourier transform infrared spectroscopy (FTIR).
Conventional sampling is shown below which illustrates the 90° and 180° geometries common to traditional and many of today's spectrometers.
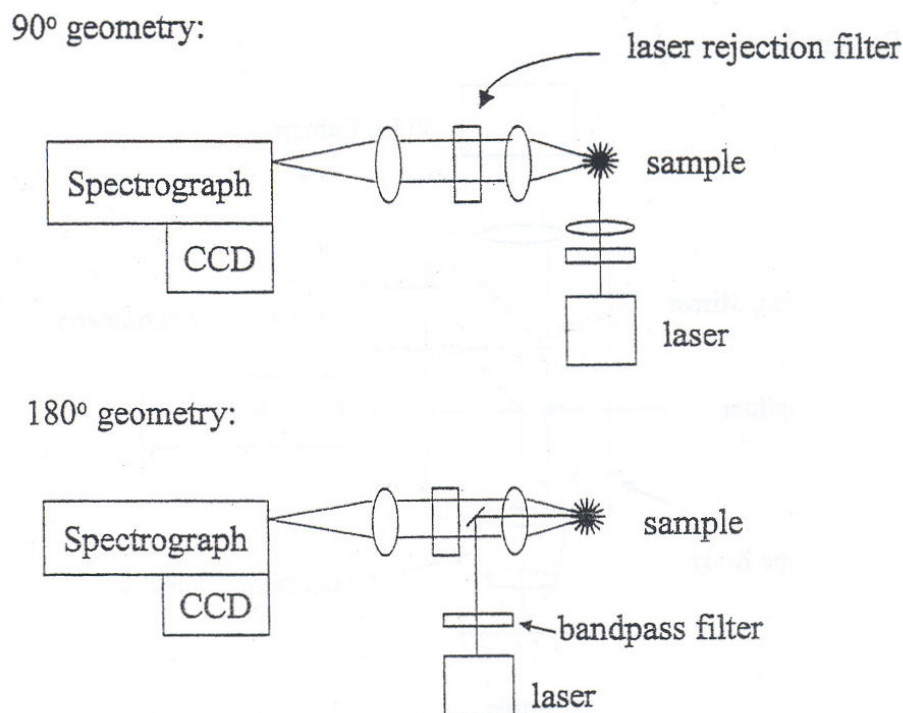
Common sampling geometries for Raman spectroscopy. Dispersive spectrometers are shown, but similar sample arrangements are used for FT-Raman.

A second general type of sampling involves *remote sampling* using fiber optics, as depicted schematically in figure below. The fiber-optic head can be quite

small and the fibers long, so Raman spectra may be obtained remotely many meters or even kilometers away from the spectrometer.

Fiber Optic Sampling:
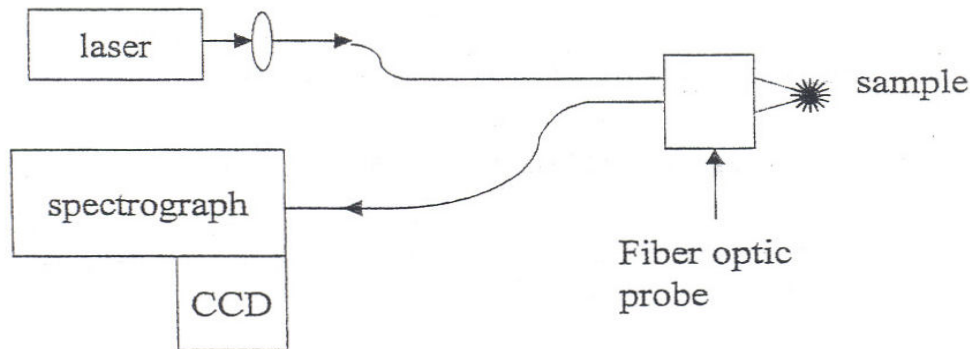
**Schematic of fiber-optic sampling configuration. Fiber lengths between probe and laser/spectrometer can be quite long, up to several hundred meters**

Applications:

-*Process monitoring*
-*Process control*
-*In a hazardous environment*
- *Analytical Raman applications*

Raman microspectroscopy is a term generally used to describe this spatially resolved technique in which spectra are obtained from microscopic domains of a sample, usually a solid or thin film. *Raman imaging* refers to techniques in which a two-dimensional image, sometimes depth resolved, is constructed using Raman scattered light.

Raman Microscope:
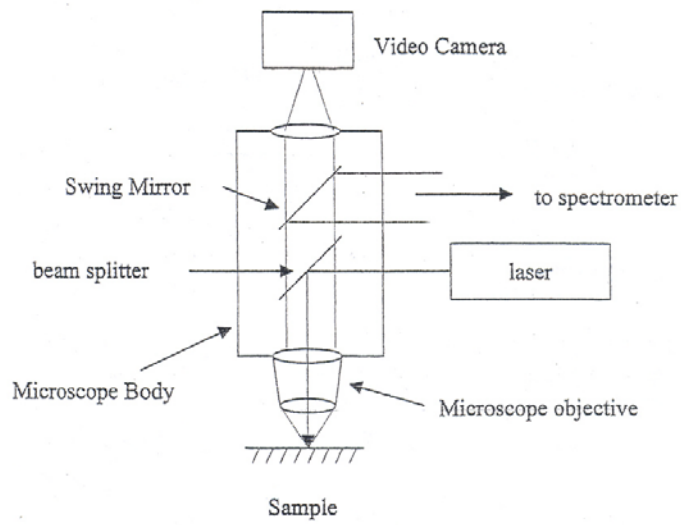
PATH LENGTH ENHANCEMENT
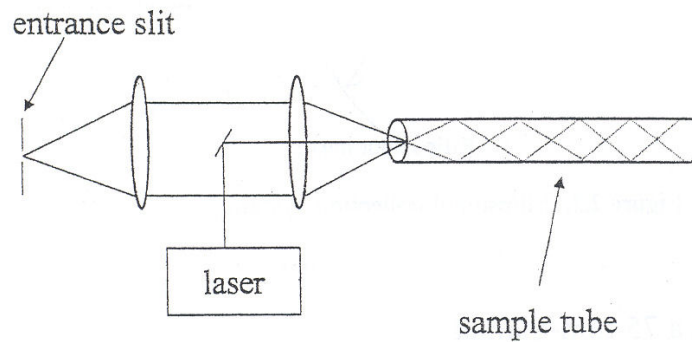
Path length enhancement for a transparent sample by reflection of laser and scattered light inside a small-diameter tube.
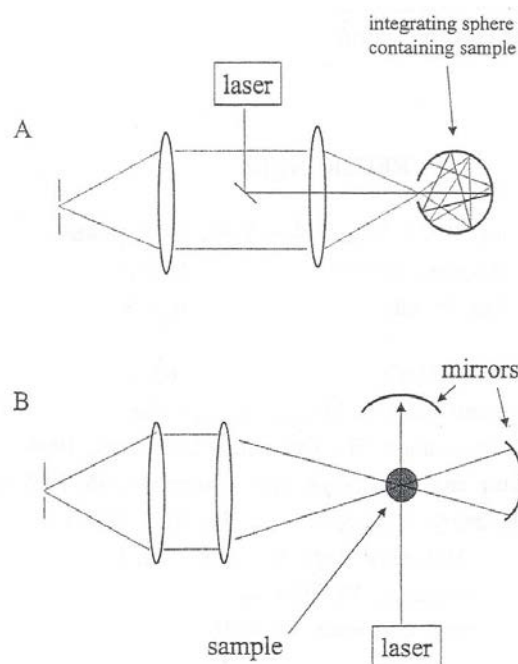
**(A) Path length enhancement for a clear sample inside an integrating sphere.**
(B) Additional mirrors to provide a double laser pass through the sample and increased collection efficiency.

References

1. L. Levi, *Applied Optics,* Vol. 1, Wiley, New York, 1968, p. 469.
2. M. Young, *Optics and Lasers,* Springer, New York, 1991, p. 206ff.
3. W. Driscoll and W. Vaughn,. eds., *Handbook of Optics,* McGraw-Hill, NewYork, 1978, pp. 14-9ff.
4. Y. W. Alsmeyer and R. L. McCreery, *Anal. Chem.,* 63, 1289 (1991).
5. M. A. Fryling, C. J. Frank and R. L McCreery, *Appl. Spectrosc.,* **47,** 1965 (1993).
6. M. A. Fryling, Ph.D. Disseration, The Ohio State University, 1994.   .
7. S. M. Angel, T. J. Kulp and T. M. Vess, *Appl. Spectrosc.,* **46,** 1085 (1992).
8. J. Zhao and R. L. McCreery, *Appl. Spectrosc.,* **51,** 1687 (1997).
9. S. D. Schwab and R. L. McCreery, *Appl. Spectrosc.,* **41,** 126 (1987).
10. D. A. Long, *Raman Spectroscopy,* McGraw-Hill, New York, 1977.
11. J. Zhao and R. L. McCreery, *Langmuir,* **11,** 4036 (1995).

3.5. LABORATORY RAMAN SPECTROSCOPY

The sample can be contained or sealed in a glass (Pyrex) tube because Raman scattered light in the visible region is not absorbed by glass.
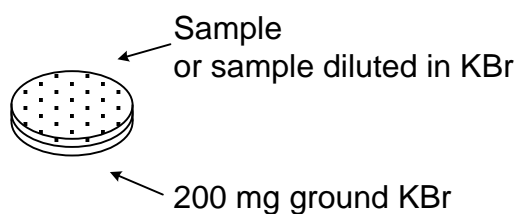

(a)   (b)   (c)
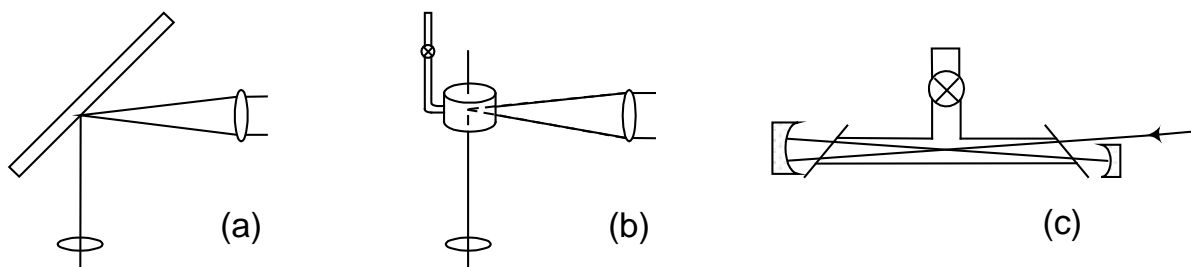
Simplest Raman cells

a, pyrex capillary for solids

b, cylindrical liquid cell

c, multipath gas cell with external resonator and Brewster windows
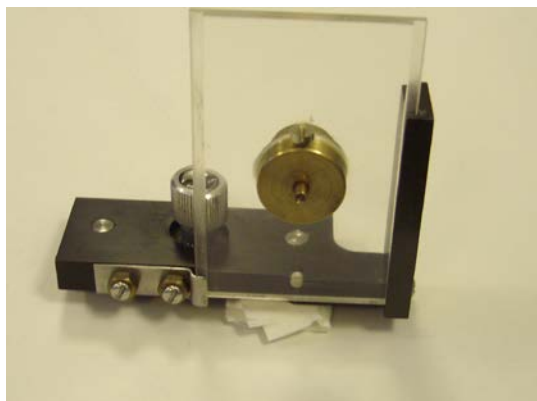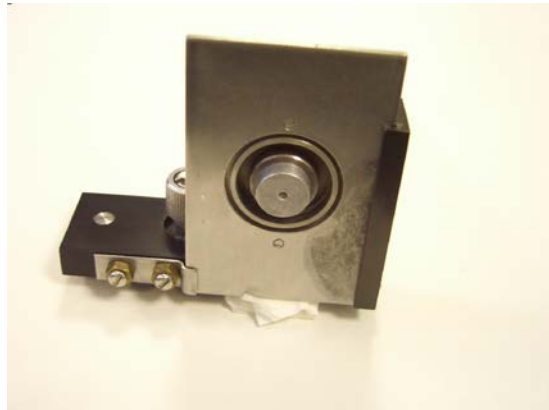
Powdered solids

KBr pel1et: 200 mg KBr+ 50 mg sample

Sample
or sample diluted in KBr

200 mg ground KBr

Laminar pel1et for front surfIace Raman scattering.

Solid sample holders I:
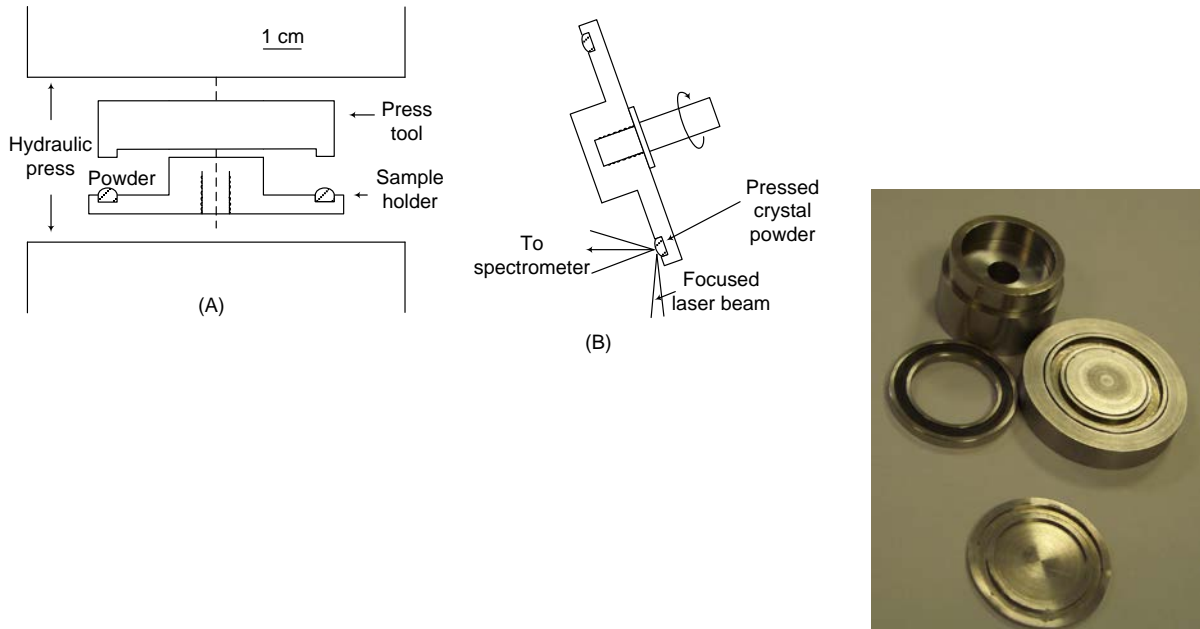(Raman spectroscopy)

Metal disks and rods with smal1 bare (1-2mm) for the powder sample. The blocks of metal reduce the sample heating.

MWNT FT-Raman spectra

MWNT FT-Raman spectra (KBr pellet)

Solid (rotating) sample holder II:
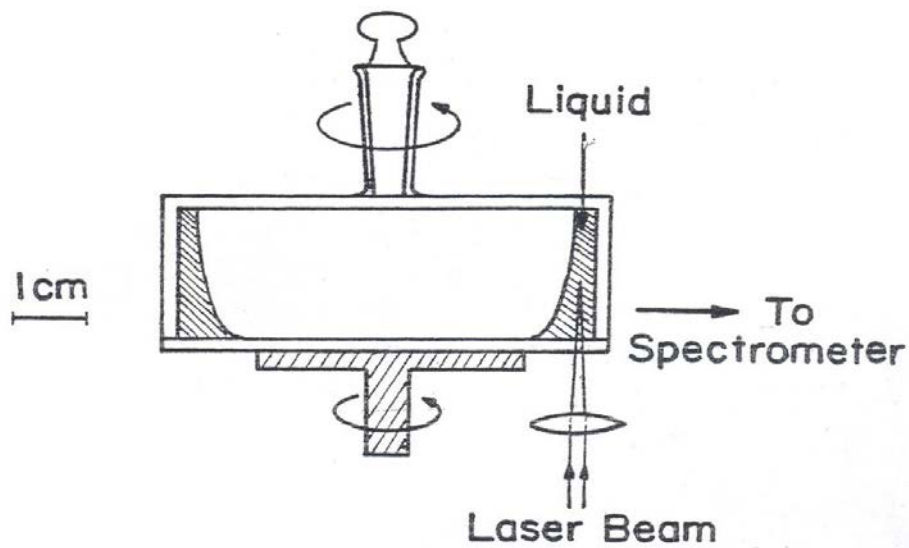(Raman spectroscopy)

(A) Sample holder with powder in ring in hydraulic press
(B) Rotating accessory in position in spectrometer

Rotating sample holder for powdered sample
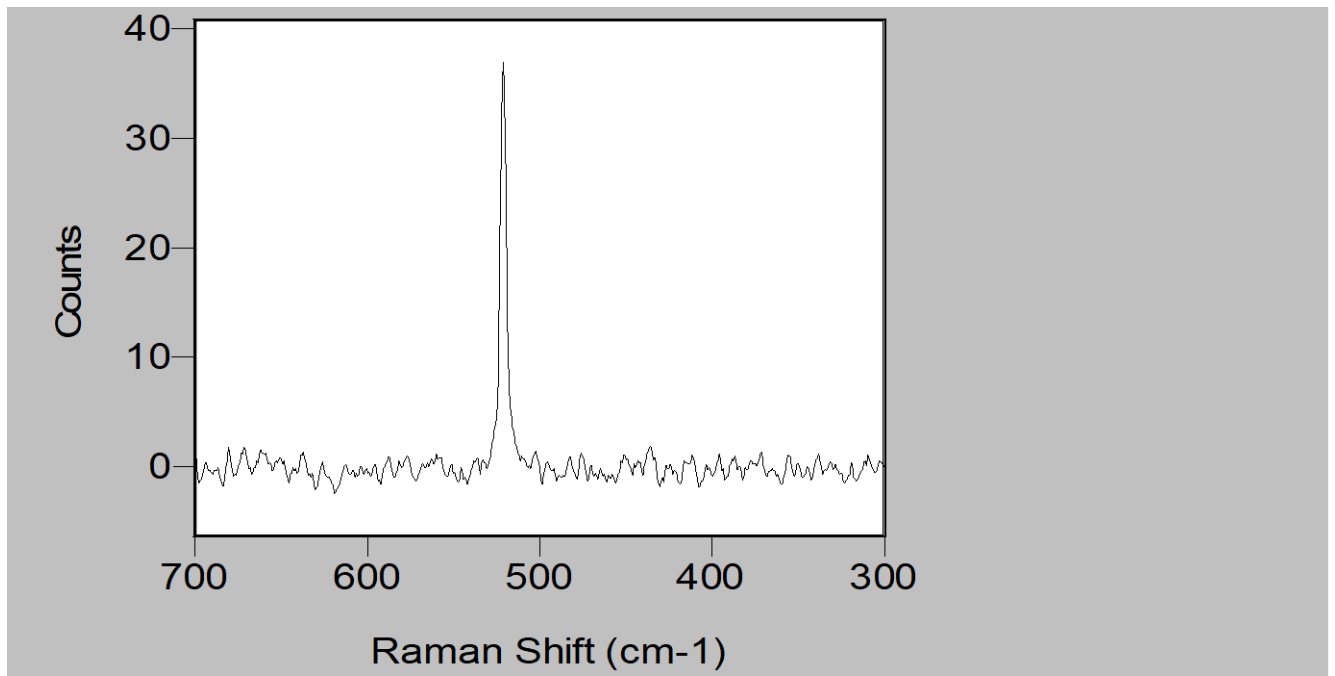
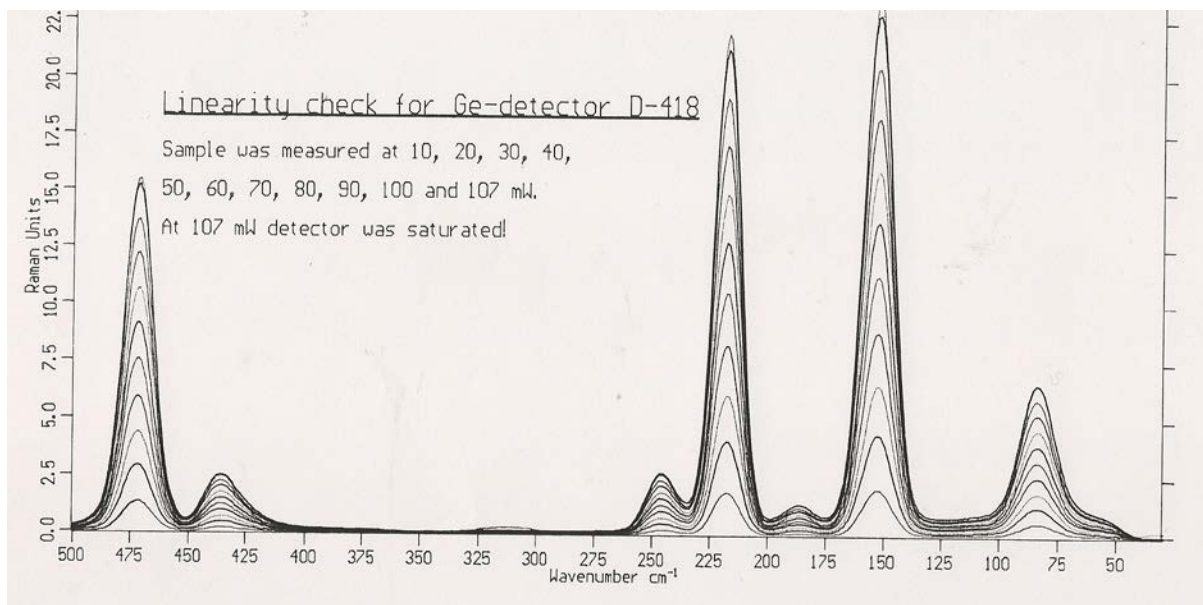## Rotating liquid cell:

Rotating Liquid sample holder

Sample high pressure, high and low temperature calls are also available (see special literature)
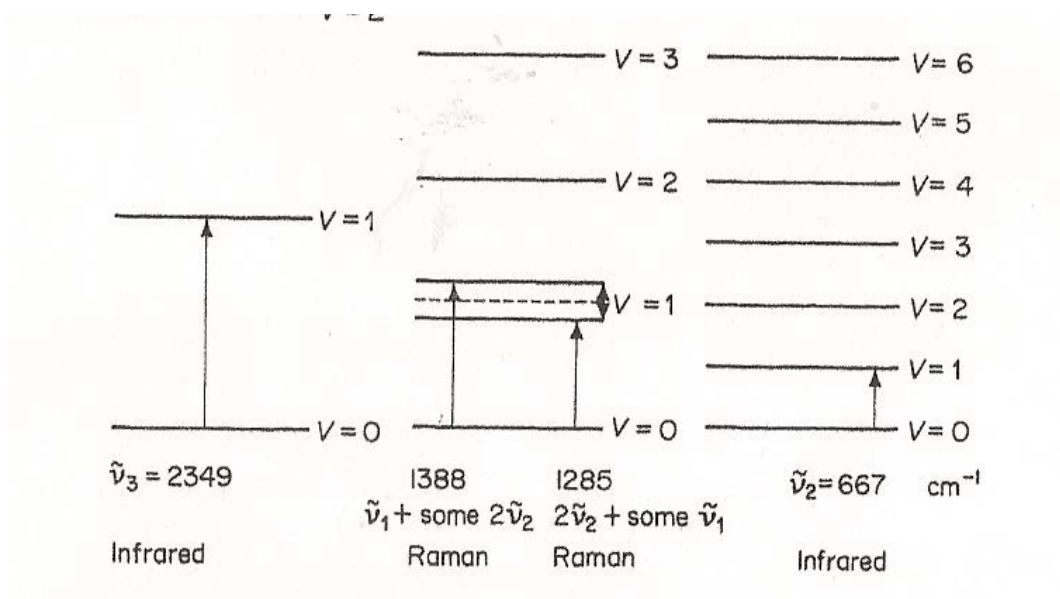
3.6. Calibration of Raman spectrometers

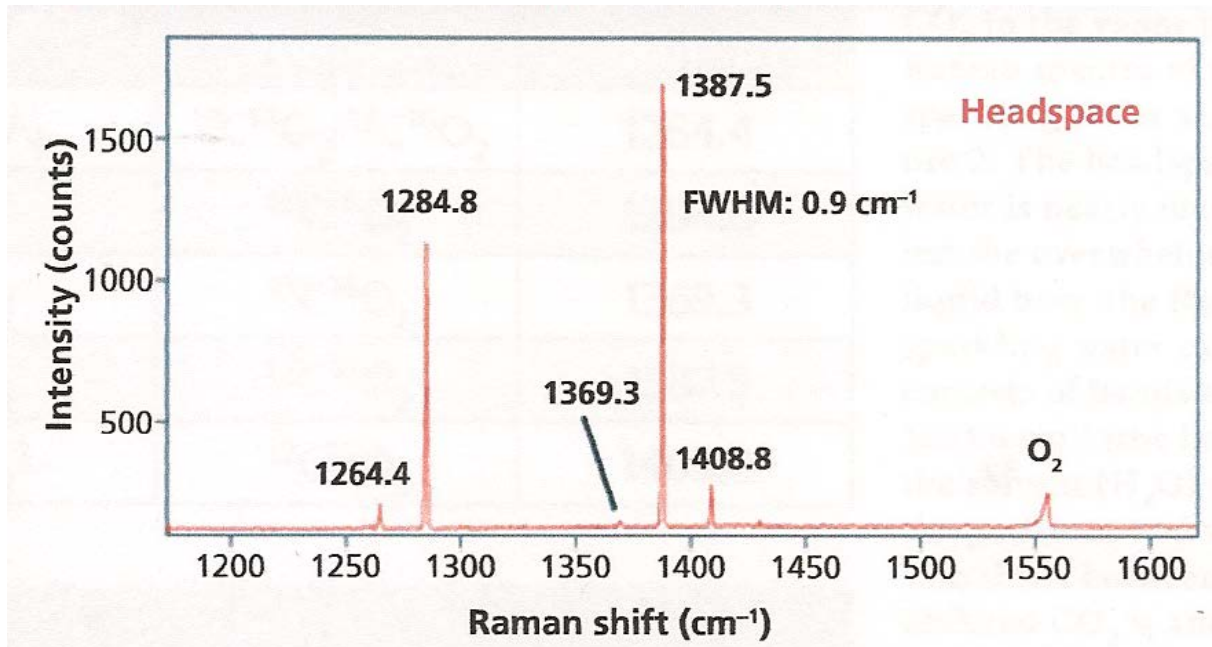**Raman microscope spectrum of silicon plate (band at 521.4 cm^{-1})**

FT-Raman spectra of solid sulphur (S$_8$). The strongest band positions are: 85.1, 153.8, 219.1, 473.2 cm^{-1}.

3.7 Fermi resonance
(E. Fermi, *Z. Phys*. 1931, 71, 250)

$\tilde{\nu}_3 = 2349$ 1388   1285 $\tilde{\nu}_2 = 667$ cm^{-1}

$\tilde{\nu}_1 +$ some $2\tilde{\nu}_2$ $2\tilde{\nu}_2 +$ some $\tilde{\nu}_1$

Infrared   Raman   Raman   Infrared

Vibrational energy levels of carbon dioxide

"Low" resolution Raman spectrum of CO_2 and O_2 (from the headspace of beer, 2014)
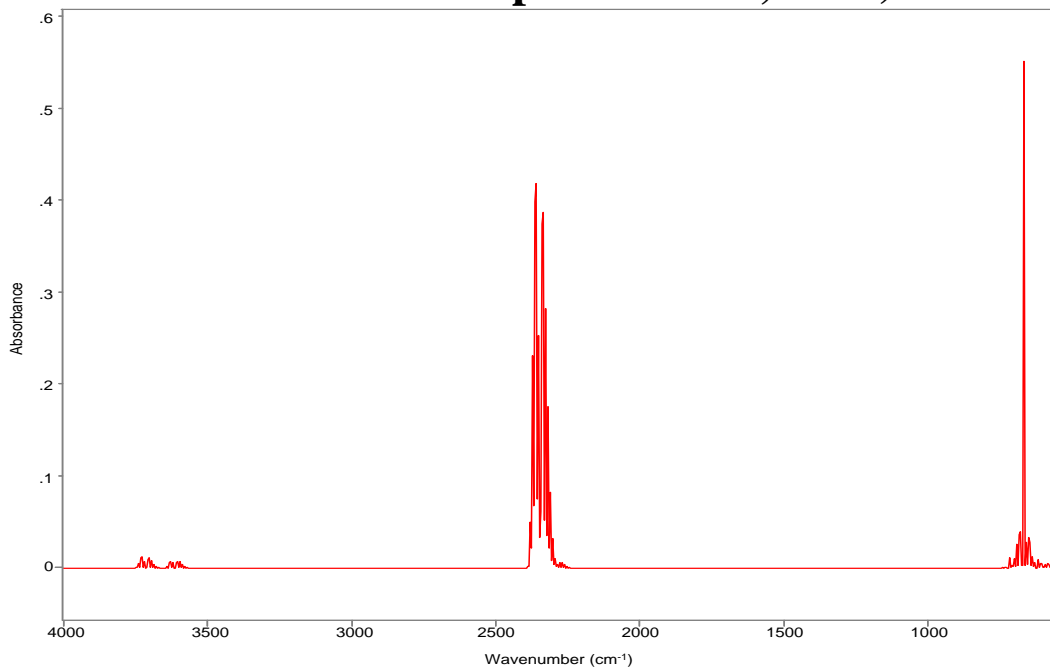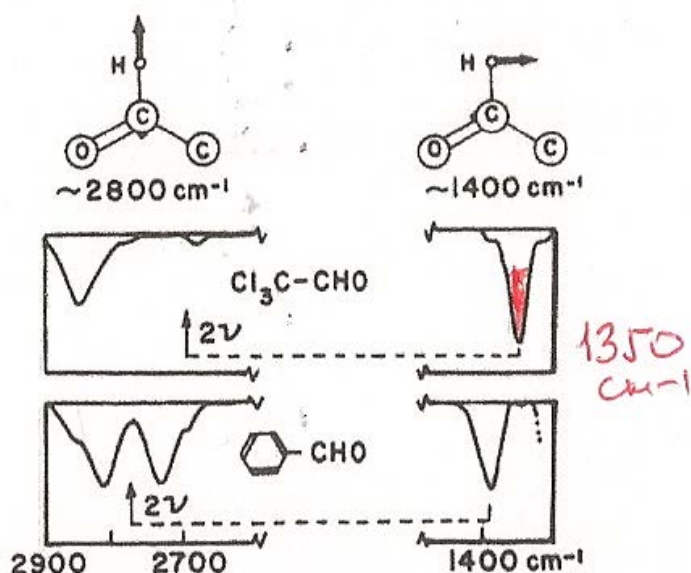

Rotational–vibrational infrared spectrum of CO_2 exhibiting parallel and perpendicular bands.

Orrection of the frequency shift:

$$\nu = 1/2\ (\nu_1 + \nu_2) \pm 1/2\ (\nu_1 - \nu_2)[(\rho-1)/(\rho +1)]$$

Here ν is the corrected wavenumber, ν_1 and ν_2 are the observed (splitted) wavenumbers, and ρ is the ratio of the observed intensities of the two bands.

~2800 cm⁻¹   ~1400 cm⁻¹

Cl_3C-CHO

2ν

1350 cm⁻¹

⬡-CHO

2ν

2900   2700   1400 cm⁻¹

Fermi resonance of C-H stretch band in benzaldehyde

IR SPECTRUM OF LIQUID ACETONIRYLE
IN CN STRETCHING REGION

Absorbance

2325   2293   225   2227

2320   2300   2280   2260   2240   2220
Wavenumber (cm-1)
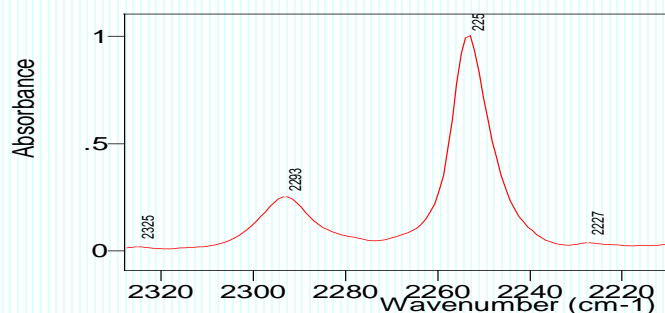
DESCRIPTION OF THE EFFECT OF FERMI RESONANCE BETWEEN FUNDAMENTAL ν_2 AND COMBINATION $\nu_3 + \nu_4$ MODES OF CH$_3$CN

2293 cm^{-1} 2253 cm^{-1}

ν_2

$\nu_3 + \nu_4$

~2270 cm^{-1}

2293   2250   cm^{-1}
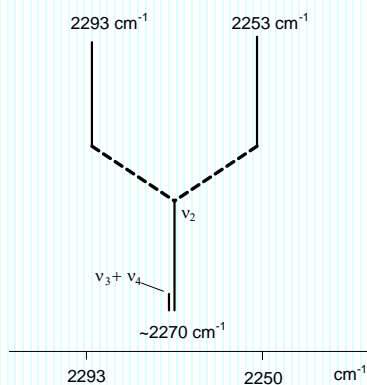
INFRARED SPECTRA OF ACETONITRILES

CH$_3$CN (liquid) cm^{-1}	CD$_3$CN (liquid) cm^{-1}	Assignments	Raman polarization
3003 (21) [a]	2258 (54)	E, ν_5, CH$_3$ asym str	dp
2943 (21)	2116 (5)	A$_1$, ν_1, CH$_3$ sym str	p
2293 (31)*	1932 (2)	A$_1$, $\nu_3 + \nu_4$, combination, (tentative assignment)	p
2253 (100)*	2262 (100)	A$_1$, ν_2, CN strech (tentative assignment)	p
1444 (52)*	1038 (24)	E, ν_6, CH$_3$ asym def (tentative assignment)	dp
1420 (45)*	1193 (7)	E, $\nu_7 + \nu_8$, combination (tentative assignment)	dp
1375 (59)	1101 (14)	A$_1$, ν_3, CH$_3$ umbrella	p
1038 (38)	847 (12)	E, ν_7, CH$_3$ rocking	dp
918 (30)	832 (27)	A$_1$, ν_4, CC strech	p
749 (14)	687 (9)	A$_1$, $2\nu_8$, overtone	p
378 (22)	348 (31)	E, ν_8, CCN bending	dp

[a] The relative intensities are is brackets;
* Unusual effects of Fermi resonance (see text)

188